

DEVELOPMENT OF THE TAYLOR DISPERSION METHOD FOR DIFFUSION COEFFICIENT MEASUREMENTS

Thesis by

Anna Zagożdżon

prepared under supervision of

prof. dr hab. Robert Hołyst

Institute of Physical Chemistry of the Polish Academy of Sciences

dr hab. Renata Małgorzata Gadzała-Kopciuch, prof. UMK

Nicolaus Copernicus University in Toruń

This dissertation was prepared within the International PhD Studies
at the Institute of Physical Chemistry of the Polish Academy of Sciences

Department of Soft Condensed Matter and Fluids

Kasprzaka 44/52, 01-224 Warsaw



Warsaw, January 2016

A-21-7

U-9-186

U-9-169

Biblioteka Instytutu Chemii Fizycznej PAN

F-B.488/16



40000000199252

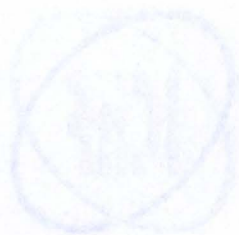
THE TAYLOR DISPERSION
FUSION COEFFICIENT
MEASUREMENTS



B. 488/16

prepared under supervision of
Prof. dr hab. Robert Holyst
Institute of Physical Chemistry of the Polish Academy of Sciences
Dr hab. Renata Makgornik-Gabaińska-Kopciuch, prof. UWIK
Nicolaus Copernicus University in Toruń
This dissertation was prepared within the International PhD Studies
at the Institute of Physical Chemistry of the Polish Academy of Sciences
Department of Soft Condensed Matter and Polymers
Kopciuch Renata 0-234 Warsaw

2-2-3
2-8-2008
2-1-2008



Warsaw, January 2016

Acknowledgements

First I would like to thank my advisor, prof. dr hab. Robert Hołyst, for sharing his knowledge and experience, his confidence in me and wise comments during our discussions. His ideas, energy and enthusiasm for the project proved to be invaluable.

I wish to express my gratitude to dr hab. Renata Gadzała-Kopciuch for her valuable comments and support.

I would like to acknowledge all colleagues from Department III for creating the friendly and highly professional environment. In particular I would like to thank Aldona Jelińska, dr Marcin Tabaka, dr Ania Ochab-Marcinek, dr Monika Asztemborska, dr Krzysiek Sozański, dr Tomek Kalwarczyk and dr Janek Paczesny.

My everlasting gratitude goes to my Parents for taking care of my education and encouraging me to follow my dreams.

I would also like to thank my husband, Damian. His love, support and encouragement allowed me to persevere in achieving my goals.

This work was supported by the National Science Centre within Opus 4 grant (UMO-2012/07/B/ST4/01400).



NATIONAL SCIENCE CENTRE

Publications connected with the thesis:

1. Lewandowska, A., Majcher, A., Ochab-Marcinek, A., Tabaka, M., Hołyst, R. *Anal. Chem.* **85**, 4051–4056 (2013).
2. Majcher, A., Lewandowska, A., Herold, F., Stefanowicz, J., Słowiński, T., Mazurek, A. P., Wieczorek, S. A., Hołyst, R. *Anal. Chim. Acta*, **855**, 51-59 (2015).
3. Zagożdżon, A., Jelińska, A., Wiśniewska, A., Górecki, M., Frelek, J., Hołyst, R. Taylor Dispersion Analysis for studying denaturation of proteins by surfactants – in preparation

Patents and patent applications:

3. Lewandowska, A., Majcher, A., Ochab-Marcinek, A., Tabaka, M., Hołyst, R. **Patent** (P-220250)
4. Majcher, A., Lewandowska, A., Hołyst, R. **Patent application** (P-407087)

Other publications:

5. Zhang, X., Poniewierski, A., Jelińska, A., Zagożdżon, A., Wieczorek, S. A., Hou, S., Hołyst, R. Evaluating the Equilibrium and Rate Constants of Noncovalent Interactions by Fluorescence Correlation Spectroscopy – in preparation
6. Domańska, U., Zawadzki, M., Królikowski, M., Lewandowska, A. *Chem. Eng. J.* **181-182**, 63-71 (2012).
6. Domańska, U., Zawadzki, M., Lewandowska, A. *J. Chem. Thermodyn.* **48**, 101-111 (2012).

Table of contents

List of publications.....	5
Table of contents.....	7
Nomenclature and abbreviations.....	9
Abstract.....	13

The literature part

1. Introduction	17
1.1. Diffusion.....	17
1.2. Application of diffusion phenomenon	18
1.3. Methods of measuring the diffusion coefficients	18
1.3.1. Diaphragm Cell.....	19
1.3.2. Dynamic Light Scattering.....	20
1.3.3. Fluorescence Correlation Spectroscopy.....	23
1.3.4. Spin Echo Nuclear Magnetic Resonance.....	27
1.4. Method selection	29
2. Literature review	30
2.1. Fundamentals of the Taylor dispersion analysis	30
2.1.1. Theory of dispersive process	30
2.1.2. Conditions for the Taylor dispersion method.....	36
2.2. Comparison of straight and coiled capillaries.....	37
2.2.1. Secondary flow.....	37
2.2.2. Dispersion in a curved capillary	39
2.3. Challenges of determining the diffusion coefficient by the Taylor dispersion analysis	41

The experimental part

3. Chemicals, equipment and procedures.....	45
3.1. Materials	45
3.2. Sample preparation.....	47
3.3. Equipment.....	47
3.4. Determination of capillary radius	48
3.5. Experimental and calculation procedures.....	48
4. Results and discussion	49
4.1. Validation of the experimental solutions	49
4.1.1. Flow rate.....	50
4.1.2. Injection volume.....	52
4.1.3. Capillary length.....	53
4.2. Analyzing dispersion process in a coiled capillary at high flow rates.....	55
4.2.1. A new solution for dispersion process in a coiled capillary at high flow rates...56	
4.2.2. Test of the equation	58
4.3. Application of a modified Taylor dispersion analysis for measurement of diffusion coefficients.....	60
4.3.1. Peptides	61
4.3.2. Drugs and potential drugs.....	62
4.3.3. DNA hairpins.....	64
4.3.4. Bacteriophages	66
4.4. Study of denaturation process of proteins by surfactants	71
4.4.1. Introduction.....	71
4.4.2. Study of denaturation of proteins by surfactant using the Taylor dispersion method	75
4.4.3. Circular dichroism measurements	77
4.4.4. Dynamic light scattering measurements	80
5. Conclusions	85
6. References.....	89

Nomenclature and abbreviations

A	Background term
A_M	Effective area of the membrane
a	Area
C	Molar concentration
C_M	Concentration of the macromolecule
C_{bottom}	Concentration of solute in bottom cell chamber
C_{top}	Concentration of solute in top cell chamber
D	Molecular diffusion coefficient
d	Diameter of the capillary
G	Strength of gradient
$g_1(q, \tau)$	Autocorrelation function
$g_2(q, \tau)$	Second order autocorrelation function
h	Injection length in the capillary
I	Fluorescence intensity
J	Flux
\bar{J}	Average mass flux
k_a	Rate constant
k_B	Boltzmann constant
L	Length of the capillary
l	Effective length of the membrane
M	Molar mass
m_1	Correction for the cross section of the rectangular injection

m_2	Correction for the cross section of the rectangular injection
N	Number of particles
$P(t)$	Normalized concentration distribution
R	Radius of the capillary
R_c	Radius of curvature of the path of the capillary
R_h	Hydrodynamic radius of the molecule
r	Coordinate in the radius direction
r_{AB}	Sum of atomic radii of A and B molecules
T	Temperature
T_2	Spin relaxation time of the species
t	Time
U	Velocity of the carrier phase
\bar{U}	Average velocity of laminar flow in the tube
V_{inj}	Volume of injection
V_{cap}	Volume of the capillary
w_{xy}	Width in the xy-plane of the confocal volume
x	Coordinates in the axial directions
z_0	Length of the confocal volume
β	Cell constant
η	Viscosity
γ	Gyromagnetic ratio
ρ	Density
σ	Dispersion coefficient
q	Scattering vector

λ	Wavelength
θ	Angle at which scattered light is detected
Γ	Decay constant
τ	Delay time
δ	Duration of the pulse
Δ	Time separation between the pulsed-gradients
ν	Kinematic viscosity
Dn	Dean number
Pe	Peclet number
Re	Reynolds number
Sc	Schmidt number
TRIS	2-Amino-2-hydroxymethyl-propane-1,3-diol
CD	Circular dichroism
CMC	Critical micelle concentration
DLS	Dynamic light scattering
FCS	Fluorescence correlation spectroscopy
PBS	Phosphate buffered saline
PGSE NMR	Pulsed gradient spin echo nuclear magnetic resonance
RF	Radiofrequency
SDS	Sodium dodecyl sulfate
TDA	Taylor dispersion analysis

Abstract

Diffusion is a phenomenon present in many natural and industrial processes. The rate of diffusion is often a factor which limits the overall rate of chemical processes. The quantity describing the diffusion rate is the diffusion coefficient, required for an appropriate description of processes involving diffusion. Although several methods are used to measure diffusion coefficients, selection of the most suitable one is often a difficult task. Physicochemical properties of the sample, its amount, the accuracy of measurement or the availability of appropriate equipment can limit the applicability of the method. Therefore it is of great importance to improve the existing solutions and methods.

The aim of the research presented in this thesis is to develop the Taylor dispersion method for diffusion coefficient measurements. Increasing the accuracy of the method and decreasing the measurement time involved are the main subject of my study. In my work I have found a new equation describing the relation between the diffusion coefficient of the analyte and its concentration distribution measured as it flows through a coiled capillary.

Chapter 1 of this thesis introduces the reader to the diffusion theory and provides an overview of the existing methods for determination of diffusion coefficients. In Chapter 2, the theoretical fundamentals of the Taylor dispersion analysis and discussion concerning flow through a coiled capillary are presented. Chapter 3 contains information on the chemicals, equipment, procedures and technical details concerning the research presented. Chapter 4 includes experimental results as well as their discussion. Finally, Chapter 5 presents the conclusions of the investigation.

The literature part

1. Introduction

1.1. Diffusion

If a drop of concentrated colored solution is added to water, it will spread out gradually. After some time the solution will appear homogeneous and the process which causes the movement of the colored solution is called diffusion. Molecular diffusion occurs as a result of the thermal motion of the molecules. Diffusion can be considered a natural mechanism of the homogenization of a substance, or a mixing process. The diffusion rate depends on several factors such as solvent viscosity, molecule size and temperature. Diffusion proceeds at the highest rate in gases (about 5 cm/min), at a lower speed in liquids (about 0.05 cm/min), and at a still lower rate in solids (about 0.00001 cm/min). Diffusion is of great importance in many processes, because it often limits their overall rate.¹

The first experimental study of diffusion was conducted by Thomas Graham between 1828 and 1850.^{2,3} He performed important experiments in gases and liquids. His studies showed that diffusion in gases is many times faster than in liquids and that the diffusion rate slows down with time. In 1855, Adolf Fick proposed a quantitative description of Graham's experiments. He described the diffusion process on the same mathematical basis as Fourier's law of heat conduction or Ohm's law of electrical conduction. He assumed that the flux of the matter J_1 is proportional to the gradient of its concentration $\frac{\partial C_1}{\partial x}$ multiplied by the area across which diffusion occurs a and the proportionality factor D :⁴

$$J_1 = -aD \frac{\partial C_1}{\partial x} \quad (1.1)$$

The factor D is the diffusion coefficient. The above equation is called the Fick's first law. The negative symbol of the Fick's law denotes that flux is directed in the opposite direction to the concentration gradient.

The Fick's second law allows to predict how concentration changes with time

$$\frac{\partial C_1}{\partial t} = D \left(\frac{\partial^2 C_1}{\partial x^2} + \frac{1}{a} \frac{\partial a}{\partial x} \frac{\partial C_1}{\partial x} \right) \quad (1.2)$$

In many practical cases the diffusion phenomenon is accompanied by convection phenomenon. In fluid mechanics convection is a macroscopic flow of matter.

Convective transport can be divided into two categories: forced and natural convection. In forced convection the mechanism of this process is not connected with heat and mass transport and arises from external sources such as a pump or a blower. In natural convection the movement of fluid arises from differences in pressures across the system.⁵⁻⁷

1.2. Application of diffusion phenomenon

Diffusion phenomenon finds extensive applications in chemical engineering problems, in petrochemical and pharmaceutical industry. Many processes such as distillation, absorption, extraction, chromatographic and electrophoretic separations or chemical reactions depend on the rate of diffusion.⁸⁻¹¹ The maximum rate constant in chemical reaction for two spherical molecules A and B can be described by the Smoluchowski equation:^{12,13}

$$k_a = 4\pi(D_A + D_B)(r_A + r_B) = 4\pi D r_{AB} \quad (1.3)$$

where D_A and D_B are the diffusion constants, and r_A and r_B the radii of molecules A and B respectively. Thus D is the relative translational diffusion coefficient and r_{AB} is the sum of the atomic radii of the molecules A and B.

Knowledge of diffusion coefficients provides also information about molecular size of particles. Relation between the diffusion coefficient and hydrodynamic radius of the molecule has the following form:

$$D = \frac{k_B T}{6\pi\eta R_h} \quad (1.4)$$

where k_B is the Boltzmann constant, T is the temperature and η is the viscosity of the solution. This equation is called the Sutherland-Stokes-Einstein equation.¹⁴⁻¹⁶

1.3. Methods of measuring the diffusion coefficients

There are several methods for measuring the diffusion coefficients. Among them the most popular are the diaphragm cell, dynamic light scattering, Taylor dispersion analysis, fluorescence correlation spectroscopy and spin echo nuclear

magnetic resonance. This chapter presents a short review of these methods. The Taylor dispersion method is described in a separate chapter as it constitutes the subject of this thesis.

1.3.1. Diaphragm Cell

The diaphragm cell is a relatively simple method of determining the diffusion coefficient. Diaphragm cells are built of two chambers separated by a glass frit or by a porous membrane.

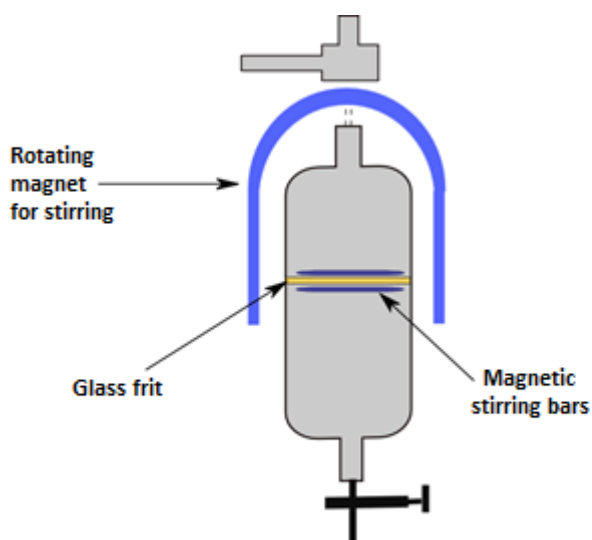


Figure 1.1. Scheme of a diaphragm cell.

These chambers are filled with solutions at different concentrations. After a certain period of time samples from both chambers are taken to measure the concentration differences.¹⁷⁻¹⁹ The diffusion coefficient is calculated from the following equation:

$$D = \frac{1}{\beta t} \ln \left[\frac{(C_{\text{bottom}} - C_{\text{top}})_{\text{initial}}}{(C_{\text{bottom}} - C_{\text{top}})_{\text{at time } t}} \right] \quad (1.5)$$

where: β is a cell constant, t is the time, and C_{bottom} and C_{top} are the concentrations of solute in bottom and top cell chamber respectively.

The cell constant is determined by calibrating the cell using a substance of known diffusion coefficient:²⁰⁻²²

$$\beta = \frac{A_M}{l} \left(\frac{1}{V_{\text{top}}} - \frac{1}{V_{\text{bottom}}} \right) \quad (1.6)$$

where A_M is the effective area of the membrane, l is the effective length of the membrane, and V_{top} and V_{bottom} are the volumes of the two cell chambers.

Benefits of diaphragm cell

- ✓ The method is simple
- ✓ The equipment is cheap (however, differences in concentrations have to be measured using other methods)

Limitations and disadvantages of diaphragm cell

- ✓ The measurement time is very long (about 48h)
- ✓ The method requires large sample volume (several mL)
- ✓ The method is occasionally unreliable (errors by an order of magnitude)

1.3.2. Dynamic Light Scattering

The next technique which allows to determine the diffusion coefficients is the Dynamic Light Scattering (DLS).²³⁻²⁵ In this method a sample is illuminated by a laser beam and the fluctuations of the scattered light at time are measured. These fluctuations are the result of Brownian motion of molecules. The intensity of the scattered light fluctuates rapidly for small molecules. To extract information from these fluctuations, the autocorrelation function is calculated with the use of digital correlator, which compares the intensity of scattered light at time t to the intensity observed at time interval τ and computes the second order autocorrelation function $g_2(q, \tau)$:²⁶⁻³⁰

$$g_2(q, \tau) = \langle I(q, t)I(q, t + \tau) \rangle \quad (1.7)$$

where q is a scattering vector given by:

$$q = \frac{4\pi n}{\lambda} \sin \frac{\theta}{2} \quad (1.8)$$

here n is the refractive index of the dispersion medium, λ is the incident laser wavelength, and θ is the angle at which scattered light is detected.

According to the Siegert equation, the second order autocorrelation function $g^2(q, \tau)$ is related to the normalized autocorrelation function $g_1(q, \tau)$:

$$g_2(q, \tau) = A + Bg_1(q, \tau) \quad (1.9)$$

A is the background term; B is the factor that depends on light scattering setup.

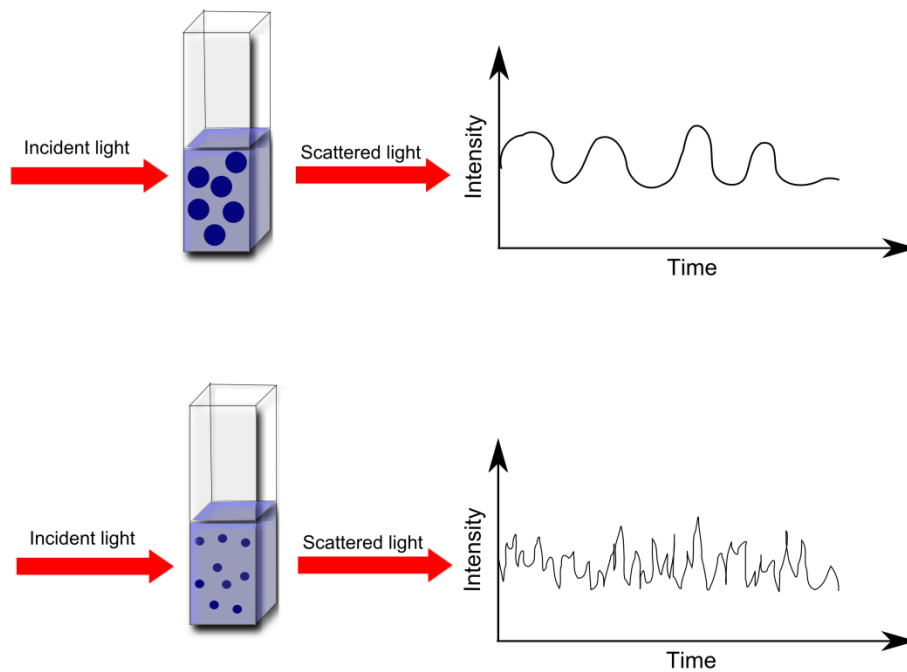


Figure 1.2. Typical intensity fluctuations for large and small particles.

If the sample is monodisperse, then the autocorrelation function $g_1(q, \tau)$ decays exponentially:²⁹⁻³⁰

$$g_1(q, \tau) = \exp(-\Gamma\tau) \quad (1.10)$$

where Γ is a decay constant

The diffusion coefficient is linearly related to Γ :

$$\Gamma = Dq^2 \quad (1.11)$$

The values of parameters A and B can be determined using a fitting program which searches for the best agreement between measured autocorrelation function and the theoretical form given by Eq. 1.10.

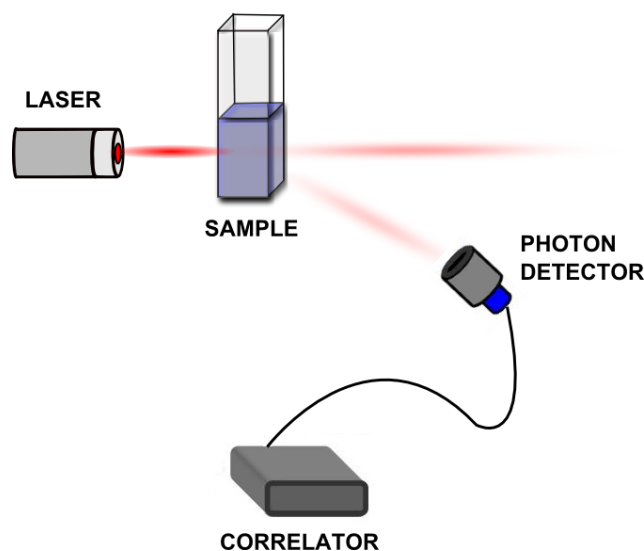


Figure 1.3. Scheme of the dynamic light scattering setup.

Benefits of dynamic light scattering

- ✓ The method allows scientists to determine the diffusion coefficient to within 2% of accuracy
- ✓ It is possible to study both small and large molecules (up to 100 nm)
- ✓ It is also possible to observe the aggregation of molecules

Limitations of dynamic light scattering

- ✓ A large volume of the sample is required (ca. 2 ml)
- ✓ A high concentration of the solute is required (concentration in the range of 10^{-5} - 10^{-3} M)
- ✓ The sample solution must be transparent
- ✓ The sample must not absorb the light of the wavelength used
- ✓ The refractive index of the studied compound and the solvent should be different
- ✓ Resolution is low – if similar-sized molecules are present in the sample, polydispersity cannot be precisely characterized
- ✓ Expensive equipment

1.3.3. Fluorescence Correlation Spectroscopy

Another method used to measure diffusion coefficients is the Fluorescence Correlation Spectroscopy (FCS).^{31,32} In this method the fluorescence intensity $I(t)$ emitted by molecules is measured. The basis of diffusion coefficient determination in FCS is the analysis of fluorescence fluctuations caused by molecules entering and leaving the observation volume (focal volume). The time which a molecule spends inside the focal volume is related to its diffusion. Thus for molecules with a large diffusion coefficient we observe faster fluctuations of fluorescence because they frequently enter and leave the focal volume.³³

From the time dependence of the fluorescence intensity the autocorrelation function $G(\tau)$ is calculated:

$$G(\tau) = \frac{\langle I(t)I(t+\tau) \rangle}{\langle I(t) \rangle^2} \quad (1.12)$$

where $\langle \dots \rangle$ is the time average of the time series signals in the equation above.

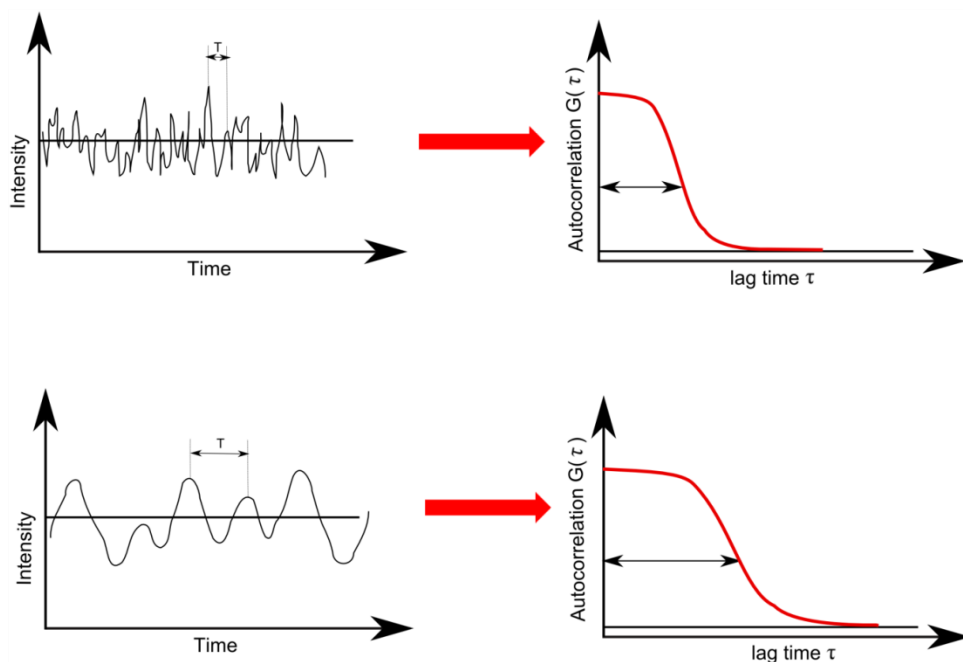


Figure 1.4. The fluorescence intensity fluctuation for fast (a) and slowly (b) moving molecules and examples of autocorrelation function.

To determine the diffusion coefficient, experimental data are fitted using theoretical models.

The form of autocorrelation function for a particle of one kind with a diffusion coefficient D and N particles in the focal volume is the following:³⁴

$$g(\tau) = 1 + \frac{1}{N} \left(1 + \frac{4D\tau}{w_{xy}^2}\right)^{-1} \left(1 + \frac{4D\tau}{z_0^2}\right)^{-1/2} \quad (1.13)$$

where w_{xy} is the width in the xy -plane and z_0 is the length of the measurement volume (z -direction). The delay time, τ , is always relative to a data point from an earlier time so that only the time difference τ is relevant.

This equation is often expressed in terms of diffusion time of the molecule in the focus τ_D :

$$g(\tau) = 1 + \frac{1}{N} \left(1 + \frac{\tau}{\tau_D}\right)^{-1} \left(1 + \frac{\tau}{\gamma^2 \tau_D}\right)^{-1/2} \quad (1.14)$$

$$D = \frac{w_{xy}^2}{4\tau_D} \quad (1.15)$$

$$\gamma = \frac{z_0}{w_{xy}} \quad (1.16)$$

To determine the diffusion coefficient, two parameters describing lateral and axial extent of the confocal volume have to be known. These parameters are determined by calibration experiment with a substance of known diffusion coefficient. This calibration has to be performed every time before measurement.

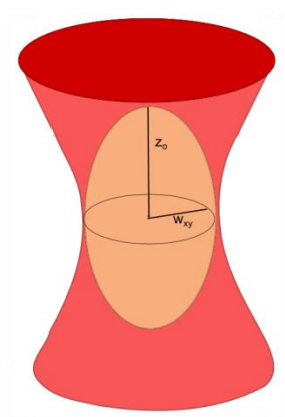


Figure 1.5. The model of confocal volume. The molecules which diffuse into this volume are excited by laser beam and emit fluorescence.

A typical FCS setup consists of a laser, an inverted microscope, a dichroic mirror, optical units and a detector (an avalanche photodiode or a photomultiplier). The exciting radiation provided by a laser beam is focused by an objective lens into the sample. The molecules in the sample are excited and emit fluorescent light. The light from the sample passes through the inverted microscope and dichroic mirror. The dichroic mirror causes separation of the excitation light from the emitted fluorescence light. Next, the fluorescence light passes through a pinhole, which blocks any fluorescence light not originating from the focal region. Then the intensity of the filtered light is measured by the detector. A schematic presentation of a confocal microscope setup is shown in Figure 1.6.

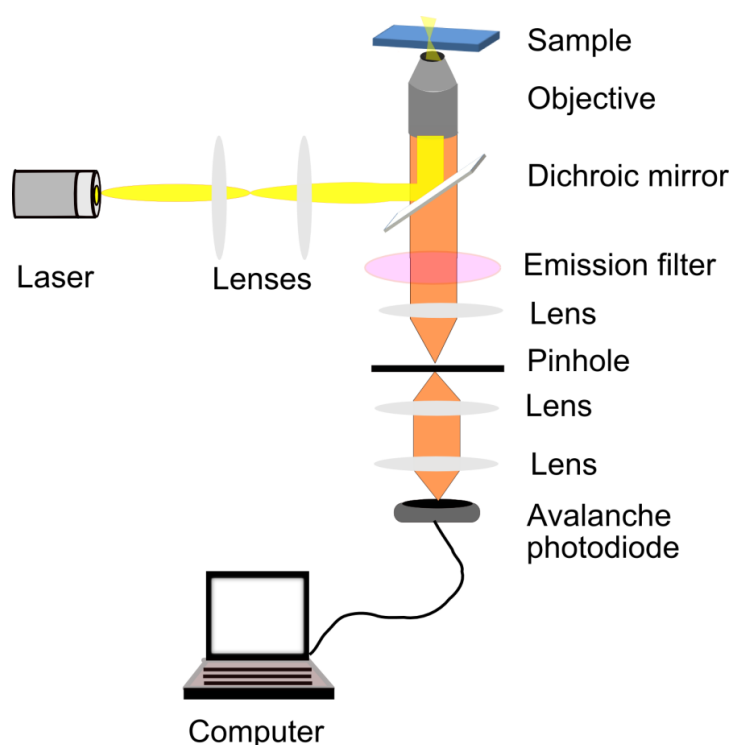


Figure 1.6. Schematic illustration of an FCS setup.

Benefits of fluorescence correlation spectroscopy

- ✓ A small sample volume is required (about 200 μ l)
- ✓ The concentration of the analyte can be very low (nanomolar)
- ✓ The time of measurement is short (several minutes)
- ✓ It can be applied to any fluorescently labeled molecules in solution, on membranes and even inside living cells

Limitations and disadvantages of fluorescence correlation spectroscopy

- ✓ The molecule of interest should be fluorescent at the applied wavelength or multiple labeling techniques should be used
- ✓ Calibration using suitable standards is necessary before measurements
- ✓ There are problems with finding suitable standards which would allow scientists to measure the standard and the investigated sample under the same conditions
- ✓ The method is sensitive to changes in confocal volume
- ✓ The equipment is very expensive
- ✓ The margin of error involved in the determination of the diffusion coefficient can amount to several percent

1.3.4. Spin Echo Nuclear Magnetic Resonance

Molecular diffusion can be measured by the pulsed gradient spin echo (PGSE) NMR technique.³⁵⁻⁴¹ In this technique two identical gradient pulses (equal in magnitude and duration) are applied, one into each period τ of the spin-echo sequence.

The idea of the diffusion measurements by PGSE NMR can be shortly described as follows. In the beginning a homogenous sample is placed in a large magnetic field to align the magnetic moments of the atomic nuclei. Then the net magnetization is oriented along the z-axis and is parallel to the external field. Next a 90° radiofrequency (RF) pulse is applied, which makes the magnetization rotate from the z-axis to the x-y plane so that it now lies along the y axis. At the point t_1 a pulse gradient is applied and then the phase shift of each spin follows. Next, a 180° radiofrequency pulse is applied along the y direction. This pulse results in inversion of the sign of the precession and phase angle. The next step is application of the second gradient at time $t_1 + \Delta$.⁴¹⁻⁴⁵ If the spins do not change positions during the experiment, they will recluster completely, forming a spin echo. However, if the diffusion is present, the precession rates will change. Consequently, not all spins refocus, and the echo signal is smaller. Therefore, the larger diffusion the smaller echo signal is observed. The stronger and longer the phase of the pulsed gradients or the longer time intervals between the pulsed gradients, the smaller the echo intensity will be.⁴¹

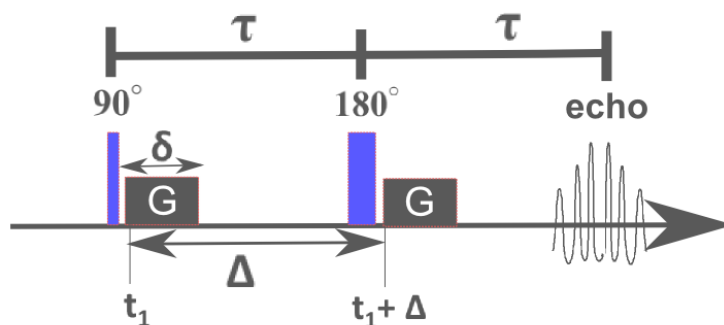


Figure 1.7. PGSE NMR pulse sequence for the diffusion measurements.

The signal intensity for a single free-diffusing component after time 2τ is given by:⁴⁵

$$I_{(2\tau,G)} = I_{(0,0)} \exp\left(\frac{-2\tau}{T_2}\right) \exp(-\gamma^2 G^2 \delta^2 (\Delta - \delta/3) D) = I_{(2\tau,0)} \exp(-\gamma^2 G^2 \delta^2 (\Delta - \delta/3) D) \quad (1.17)$$

where $I_{(0,0)}$ is the signal intensity immediately after 90° RF pulse, T_2 is the spin-spin relaxation time of the species, γ is the gyromagnetic ratio, G is the strength of the applied gradient, δ is the duration of the pulse, Δ is the time separation between the pulsed-gradients and D is the diffusion coefficient.

From this equation we get:⁴⁵

$$\ln\left(\frac{I_{(2\tau,G)}}{I_{(2\tau,0)}}\right) = (-\gamma^2 G^2 \delta^2 (\Delta - \delta/3) D) = -bD \quad (1.18)$$

To determine the diffusion coefficients, a series of experiments should be conducted, in which different values of the field gradient strength or the duration of the pulse are applied, while the other parameters are kept constant. Next, the $\ln(I_{(2\tau,G)}/I_{(2\tau,0)})$ should be plotted versus the b . From the slope of straight line we obtain the value of the diffusion coefficient.

Benefits of pulsed gradient spin echo (PGSE) NMR

- ✓ It is a completely non-invasive technique
- ✓ The margin of error involved in the accuracy of determining diffusion coefficients is around five percent

Limitations and disadvantages of pulsed gradient spin echo (PGSE) NMR

- ✓ It is necessary to use deuterated solvents
- ✓ The method is sensitive to the phase instability of the spectrometer
- ✓ The method is sensitive to mismatching of the gradient pulse time integrals
- ✓ The method is sensitive to vibrations of the sample

1.4. Method selection

Selection of the appropriate method of measuring diffusion coefficients depends on many factors such as concentration and volume of the sample, physicochemical properties of the studied compounds, the time of measurement and the accuracy etc. The choice of method is not subject to any hard and fast rule. Therefore, method selection is often based on a comparison of the benefits and limitations of each technique and on the knowledge of the researcher. This section briefly describes the main factors which need to be taken into account when selecting the method.

The first consideration is the concentration and volume of the sample. There are situations in which only a small amount of the sample is available or solubility is very low and more substance cannot be dissolved. In this case it is necessary to apply a highly sensitive detection system (for example fluorescence detection). The next important consideration is the range of the diffusion coefficients which can be measured using a particular method. Another crucial condition during the selection process is the complexity of the method as some of them require special preparation of the sample and involve multiple stages. Sometimes an analysis of experiment results is difficult, laborious and requires a very experienced professional thus simplicity is clearly most desirable. Yet another important factor is equipment availability and cost. Finally, the time constraints of the method often need to be considered (especially with a large number of samples to test).

2. Literature review

2.1. Fundamentals of the Taylor dispersion analysis

A. Griffiths in 1911 observed that if a drop of dye solution is inserted as a marker in a stream of water flowing slowly through a capillary, the colored solution spreads out symmetrically.⁴⁶ In 1953 Sir Geoffrey Taylor proposed a mathematical model⁴⁷ describing the dispersion process observed by Griffiths. His theory found its application in determining the diffusion coefficients in liquids and was named the Taylor dispersion technique in his honor.

2.1.1. Theory of dispersive process

When a fluid is flowing with Poiseuille laminar flow through a circular capillary, the velocity over the cross section has a parabolic profile (Fig. 2.1). The parabolic velocity profile can be described as follows:

$$U'(r) = \bar{U} \left(1 - 2 \left(\frac{r}{R} \right)^2 \right) \quad (2.1)$$

where \bar{U} is the average flow velocity, r is the coordinate in the radius direction, and R is the radius of the capillary. It means that molecules in the center of the capillary move faster than molecules close to the walls.

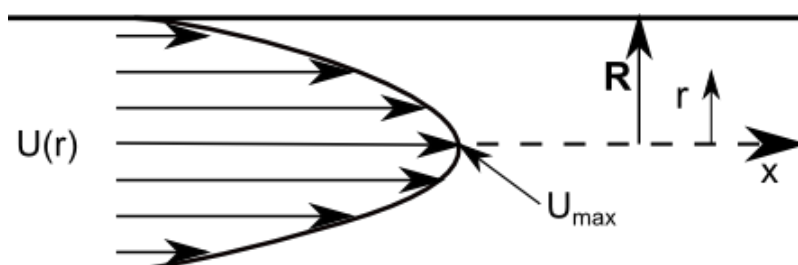


Figure 2.1. Schematic presentation of the Poiseuille laminar flow.

If we inject the compound of interest into the flow, we would expect concentration distribution to be asymmetrical due to parabolic convection. However, the final concentration distribution is symmetrical. Taylor explained this phenomenon as an effect of action of convection and radial diffusion.^{47,48} After injection of the solution into the carrier phase, the plug takes a parabolic shape due to Poiseuille flow. Then radial diffusion starts to work due to the concentration gradient. The molecules from the front part of sample diffuse from the center of the capillary to the capillary walls and the molecules from the back part of sample diffuse from the walls to the capillary center. Therefore after some time we obtain symmetrical concentration distribution of the sample.

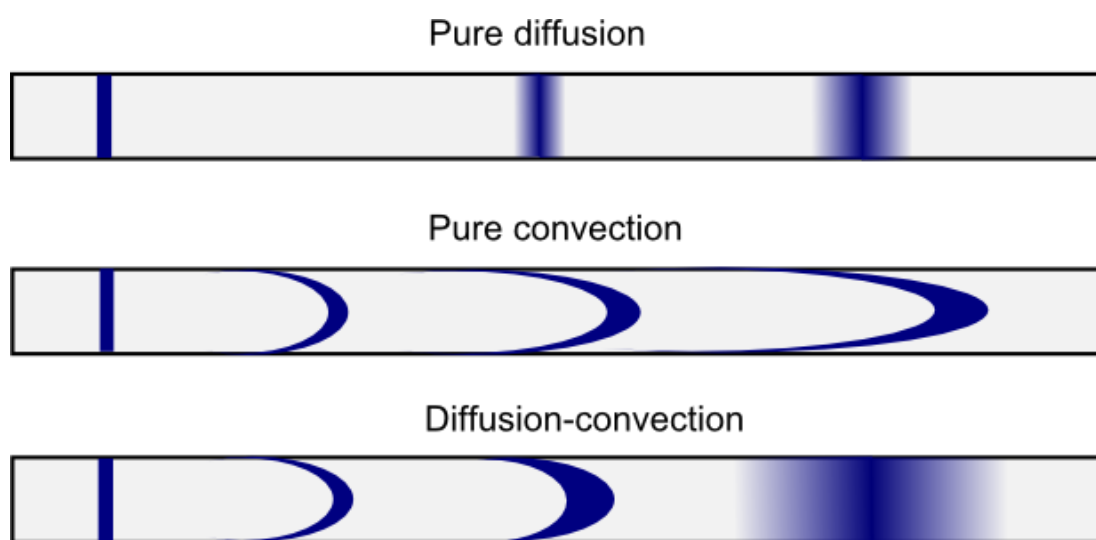


Figure 2.2. Illustration of dispersion process by diffusion alone (a), convection alone (b) and diffusion and convection (c).

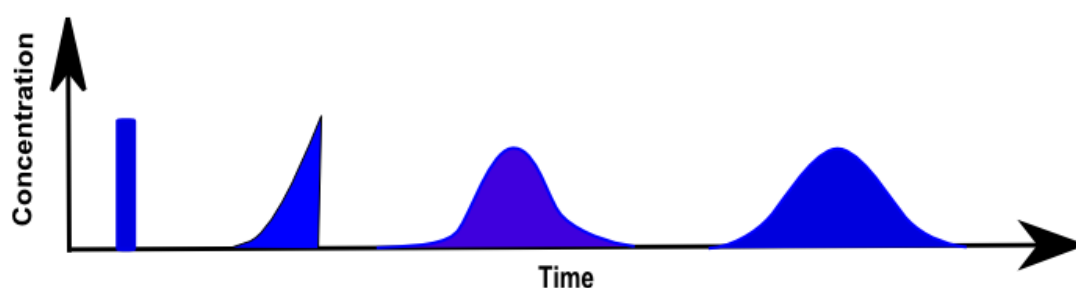


Figure 2.3. Concentration profile of the analyte at different points in time during its flow through a capillary.

In case of flow through a capillary the convection-diffusion equation has the following form:^{47,48,49,50}

$$\frac{\partial C}{\partial t} + 2\bar{U} \left(1 - \left(\frac{r}{R}\right)^2\right) \frac{\partial C}{\partial x} = D \left(\frac{1}{r} \frac{\partial}{\partial r} \left(r \frac{\partial C}{\partial r}\right)\right) + D \left(\frac{\partial^2 C}{\partial x^2}\right) \quad (2.2)$$

Due to the fact that carrier phase moves by Poiseuille laminar flow, Eq. 2.2 has two boundary conditions in the radial direction:

$$\frac{\partial C}{\partial r} = 0, \quad r = R \quad (2.3.)$$

$$\frac{\partial C}{\partial r} = 0, \quad r = 0 \quad (2.4)$$

The mixed zone is moving continuously; therefore we can consider a new axial coordinate x'

$$x' = x - \bar{U}t \quad (2.5)$$

After substituting $x = x' + \bar{U}t$ into Eq. 2.2 we obtain:

$$\frac{\partial C}{\partial t} + \bar{U} \left(1 - 2\left(\frac{r}{R}\right)^2\right) \frac{\partial C}{\partial x'} = D \left(\frac{1}{r} \frac{\partial}{\partial r} \left(r \frac{\partial C}{\partial r}\right)\right) + D \left(\frac{\partial^2 C}{\partial x'^2}\right) \quad (2.6)$$

In order to obtain an approximate analytical solution of Eq. 2.6 Taylor made the following assumptions:

- ✓ the axial diffusion is small compared with convection term:

$$\bar{U} \left(1 - 2\left(\frac{r}{R}\right)^2\right) \frac{\partial C}{\partial x'} \gg D \left(\frac{\partial^2 C}{\partial x'^2}\right), \text{ thus } D \left(\frac{\partial^2 C}{\partial x'^2}\right) = 0 \quad (2.7)$$

- ✓ the radial diffusion has enough time to eliminate anomalies in radial concentration distribution due to convection, thus

$$\frac{\partial C}{\partial t} \approx 0 \quad (2.8)$$

After taking into account these assumptions, Eq. 2.6 takes the following form:

$$\frac{\partial}{\partial r} \left(r \frac{\partial C}{\partial r} \right) = \frac{\bar{U}}{D} \left(1 - 2 \left(\frac{r}{R} \right)^2 \right) r \frac{\partial C}{\partial x'} \quad (2.9)$$

Integrating the above equation twice with respect to r results in:

$$C(r) = \frac{\bar{U}}{D} \left(\frac{r^2}{4} - \frac{r^4}{8R^2} \right) \frac{\partial C}{\partial x'} + \varepsilon \ln r + \kappa \quad (2.10)$$

where ε and κ are constants of integration. Due to the boundary condition:

$$\frac{\partial C}{\partial r} = 0, \quad r = 0$$

we assume that ε is 0, because otherwise $C \rightarrow \infty$ which is physically impossible.

Then we obtain:

$$C(r) = \frac{\bar{U}R^2}{4D} \frac{\partial C}{\partial x'} \left(\frac{r^2}{R^2} - \frac{r^4}{2R^2} \right) + \kappa = \psi \left(\frac{r^2}{R^2} - \frac{r^4}{2R^2} \right) + \kappa \quad (2.11)$$

where

$$\psi = \frac{\bar{U}R^2}{4D} \frac{\partial C}{\partial x'} \quad (2.12)$$

In the case of transport along a capillary, the average concentration over any radial cross-section is more important than local concentration. We can express the average concentration as follows:

$$\bar{C} = \frac{1}{\pi R^2} \int_0^R C \cdot 2\pi r \, dr = \frac{2}{R^2} \int_0^R cr \, dr \quad (2.13)$$

$$\bar{C} = \frac{1}{3} \psi + \kappa \quad (2.14)$$

Elimination of κ from Eq. 2.11 by substituting $\kappa = \bar{C} - \frac{1}{3} \psi$ gives:

$$C = \bar{C} + \frac{UR^2}{4D} \frac{\partial C}{\partial x'} \left(-\frac{1}{3} + \frac{r^2}{R^2} - \frac{1}{2} \frac{r^4}{R^4} \right) \quad (2.15)$$

The radial variations of concentration are small in relation to the axial ones; therefore we can assume:

$$\frac{\partial C}{\partial x'} \approx \frac{\partial \bar{C}}{\partial x'} \quad (2.16)$$

The average mass flux across any section moving with a mean speed of flow can be expressed as:

$$\bar{J} = \frac{1}{\pi R^2} \int_0^R C U' \cdot 2\pi r \, dr \quad (2.17)$$

After substituting Eq. 2.15 with Eq. 2.17 and taking into account approximation 2.16 we get:

$$\bar{J} = - \left(\frac{R^2 \bar{U}^2}{48D} \right) \frac{\partial \bar{C}}{\partial x'} \quad (2.18)$$

Term:

$$\sigma = \frac{R^2 \bar{U}^2}{48D} \quad (2.19)$$

in equation is called the dispersion coefficient and describes the axial spreading of a solute in the capillary. According to results obtained by Taylor, the larger velocity we use the greater will be the axial spreading due to convection. Otherwise, the dispersion coefficient is inversely proportional to the molecular diffusion coefficient. Thus rapid diffusion leads to small dispersion.

The conservation of mass is written as:

$$\frac{\partial \bar{C}}{\partial t} = - \frac{\partial \bar{J}}{\partial x'} \quad (2.20)$$

After substituting Eq. 2.18 into Eq. 2.20 we get the equation for longitudinal dispersion

$$\frac{\partial \bar{C}}{\partial t} = -\sigma \frac{\partial^2 \bar{C}}{\partial x'^2} \quad (2.21)$$

Taylor's considerations are based on the assumption that the axial molecular diffusion can be neglected. Several years after Taylor's publication, Aris showed that the effect of axial diffusion on dispersion coefficient σ is additive:⁵¹

$$\sigma = D + \frac{R^2 \bar{U}^2}{48D} \quad (2.22)$$

He used the method of moments and calculated the total moments of concentration $C(x, r, t)$ and the average concentration $\bar{C}(x, t)$:

$$M_n(t) = \frac{2}{R^2} \int_{-\infty}^{+\infty} x^n dx \int_0^R C(x, r, t) r dr \quad n = 0, 1, 2, \dots \quad (2.23)$$

$$\bar{M}_n(t) = \int_{-\infty}^{+\infty} x^n \bar{C}(x, t) dx \quad n = 0, 1, 2, \dots \quad (2.24)$$

The functions $M_n(t)$ were obtained from Eq. 2.2 and functions $\bar{M}_n(t)$ were obtained from Eq. 2.19. The dispersive coefficient was determined by matching the first three moments of $M_n(t)$ to $\bar{M}_n(t)$ for times $t \gg \frac{R^2}{D}$. In practice, the second term in the equation is much bigger than the axial diffusion and can be neglected.

The concentration distribution of the compound of interest at the end of the capillary is the Gaussian function. The normalized distribution has the following form:

$$P(t) = \frac{1}{2\sqrt{\pi\sigma t}} \exp \left[-\frac{(L-ut)^2}{4\sigma t} \right] \quad (2.25)$$

where σ is the dispersion coefficient [$\text{m}^2 \text{s}^{-1}$], t is time [s], L is the capillary length [m], and u is the average velocity [m s^{-1}] (averaged over the cross section of the capillary).

The concentration distribution given by Eq. 2.25 is transformed into the following form (Eq. 2.26) due to finite injection volume of the sample:^{8,52,53}

$$P(t) = \frac{1}{\sqrt{2\pi}} \frac{Ah}{\sqrt{2\sigma t + m_2}} \exp \left[-\frac{(L-ut + m_1)^2}{2(2\sigma t + m_2)} \right] \quad (2.26)$$

where A is the amplitude, u is the velocity, σ is the dispersion coefficient, h is the injection length in the capillary given by $h = LV_{inj} V_{cap}^{-1}$, where L is the capillary length, V_{inj} is the volume of injection, V_{cap} is the volume of the capillary. Parameters m_1 , m_2 denote corrections for the cross section of the rectangular injection. They are defined in the following way: $m_1 = 1 (2h)^{-1}$ and $m_2 = 1 (12h^2)^{-1}$. Consequently, we get:

$$P(t) = \frac{2\sqrt{3}}{\sqrt{2\pi}} \frac{Ah}{\sqrt{24\sigma t + h^2}} \exp \left[-\frac{6(L-ut + h/2)^2}{(24\sigma t + h^2)} \right] \quad (2.27)$$

2.1.2. Conditions for the Taylor dispersion method

To obtain symmetrical concentration distribution from which we can extract proper value of the diffusion coefficient, several conditions should be satisfied:

1. The flow of the carrier phase should be laminar, thus the Reynolds number Re should be smaller than 2000

$$Re = \frac{\rho d U}{\eta} < 2000 \quad (2.28)$$

where ρ is the density of the carrier phase, d is the diameter of the capillary, U is the velocity of the carrier phase, and η is the viscosity of the carrier phase.

2. The ratio of the injection volume V_{inj} to the capillary volume V_{cap} should be:⁵⁴

$$\frac{V_{inj}}{V_{cap}} < 0.01 \quad (2.29)$$

This condition allows us to neglect the initial shape of the pulse, because the sample has enough volume to disperse in.

3. The axial diffusion should be negligible

$$Pe = \frac{UR}{D} \gg \sqrt{48} \approx 6.9 \quad (2.30)$$

where Pe is the Peclet number.

4. The length $\frac{UR^2}{D}$ should be small compared with the length of capillary L in which changes in C appear. Thus,

$$\frac{4L}{R} \gg Pe \quad (2.31)$$

2.2. Comparison of straight and coiled capillaries

To fulfill the conditions described in the previous section, long capillaries (about 20 m) are customarily used. For practical reasons, it is beneficial to coil the capillary. This solution has a few advantages: less space is occupied, better temperature control is achieved, data communication line is shorter and the capillary is less vulnerable. However, flow through a coiled capillary differs from flow through a straight capillary as in a coiled capillary the secondary flow appears in the cross section of the coiled capillary.^{55,56} It is the effect of the force imbalance between the centrifugal force and radial pressure fields. The secondary flow increases lateral mixing and as a result reduces the longitudinal dispersion.

2.2.1. Secondary flow

During its flowing through a curved capillary with a radius of curvature R_c the fluid particles moving with velocity U experience a centrifugal force equaling mU^2/R_c . The radius of curvature of the particle paths is the greatest near the outer wall and the smallest near the inner one. Moreover, due to viscosity, the particles in the central axis move with a larger velocity than particles close to the walls. In consequence, the strongest centrifugal force acts on the fluid in the central axis and the weakest on the particles near the outer wall. A pressure gradient generated to balance the centrifugal force results in the fluid near the center of the capillary being swept towards the outer side of the bend and the fluid near the

capillary wall returning towards the inside of the bend. As a result, two vortices appear, due to which the fluid motion is not parallel to the axis of the capillary for the whole length of the capillary. These vortices are called Dean vortices after the British scientist, W.R. Dean, who first presented a systematic study of the secondary flow in coiled capillaries.^{57,58} He found dimensionless quantity defined as:

$$De = Re \sqrt{\frac{R}{R_c}} \quad (2.32)$$

where De is the Dean number, Re is the Reynolds number, R is the radius of the capillary, and R_c is the radius of curvature of the path of the capillary.

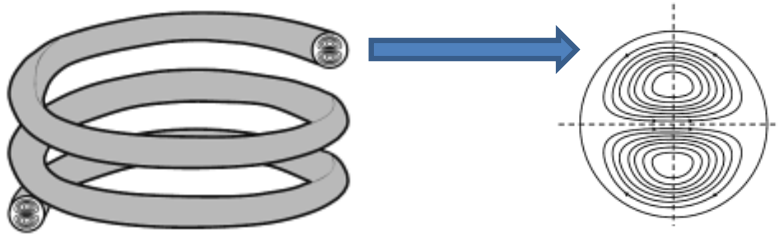


Figure 2.4. The vortices generated due to the curve path of flow in a coiled capillary (adapted from ref. 55).

Dean used a perturbation procedure to solve the Navier–Stokes equation for fully developed laminar flow in a coiled capillary for small values of the Dean number.⁵⁹ He presented a series solution as a perturbation of the parabolic velocity profile in a straight capillary. The series expansion is as follows:⁶⁰

$$\frac{U(r,\theta)}{2U^*} = 1 - \left(\frac{2r}{D}\right)^2 + \left(\frac{De^*}{96}\right)^2 \left[\frac{19}{40} \left(\frac{2r}{D}\right) - \left(\frac{2r}{D}\right)^3 + \frac{3}{4} \left(\frac{2r}{D}\right)^5 - \frac{1}{4} \left(\frac{2r}{D}\right)^7 - \frac{1}{40} \left(\frac{2r}{D}\right)^9 \right] \sin \theta \quad (2.33)$$

where U^* is the half of the maximum velocity which would be produced in a straight capillary by pressure gradient applied along the curved capillary, and De^* is the Dean number calculated using U^* . From this solution the picture of the secondary flow streamlines can be obtained.

Dean's publication was followed by many studies concerning secondary flow. White (1929) showed that Dean's theory is valid for different curvatures of the

capillary. He also pointed out that velocities of the flow at which the flow ceases to be steady and becomes turbulent are much higher for a coiled capillary than for a straight one.⁶¹ This unexpected result was confirmed by Taylor.⁶² Thus the curving of the capillary increases the stability of the flow and the transition from laminar to turbulent flow appears at a higher Reynolds number than for a straight capillary.

2.2.2. Dispersion in a curved capillary

The secondary flow mixes an analyte better in a capillary during the the Poiseuille flow. Consequently, the concentration distribution is more uniform and we observe less dispersion in comparison to the dispersion in a straight capillary. This effect was observed by Evans and Kenney (1965),⁶³ and by Caro (1966).⁶⁴ Dispersion in a curved capillary attracted considerable attention of scientists due to wide application of curved capillaries in many engineering devices. Moreover, the human circulatory and respiratory systems are composed of many curved and bifurcating vessels. Therefore impact of the secondary flow on longitudinal dispersion was investigated by many researchers. Erdogan and Chatwin⁶⁵ were the first to apply Dean's solution for the calculation of dispersion in a curved capillary while Nunge, Lin and Gill⁶⁶ used Topakoglu's⁶⁷ velocity profiles for calculation. Erdogan and Chatwin as well as Nunge, Lin and Gill relate the dispersion coefficient with the ratio of the radius of the capillary to the radius of curvature of the path of the capillary, with Reynolds number Re , and with Schmidt number, which is defined as follows:

$$Sc = \frac{\nu}{D} \quad (2.34)$$

where ν is the kinematic viscosity and D is the diffusion coefficient.

However, both solutions can be only used to predict the conditions under which the Taylor equation is valid in a curved capillary. Janssen⁶⁸ was the first to indicate that the ratio of the effective dispersion coefficient in curved and straight tubes is a function of the parameter De^2Sc . This parameter expresses the ratio of the convective and diffusive terms and is sometimes called the secondary flow Peclet

number.⁶⁹ Depending on the value of the parameter De^2Sc , curvature has different impact on the dispersion. For a small value of this parameter the centrifugal force is too small to have an effect on the flow pattern. If the De^2Sc is increased, the secondary flow gradually develops and decreases dispersion. This result explains different dispersion behaviors of gases and liquids at identical Dean numbers.

Johnson and Kamm⁷⁰ used Monte Carlo and numerical techniques for calculation of dispersion in a curved capillary at low Dean number. They made simulations for the parameter De^2Sc ranging from 1 to 10^5 . Their theory predicted that:

$$\frac{\sigma_s}{\sigma_c} = 5 \quad (2.35)$$

for $De^2Sc > 10^4$, where σ_s is the dispersion coefficient in a straight capillary and σ_c is the dispersion coefficient in a coiled capillary. In spite of the fact that the agreement between numerical and experimental results is generally good, at high values of parameter De^2Sc a discrepancy appears (it does not reach the limit suggested by the model).

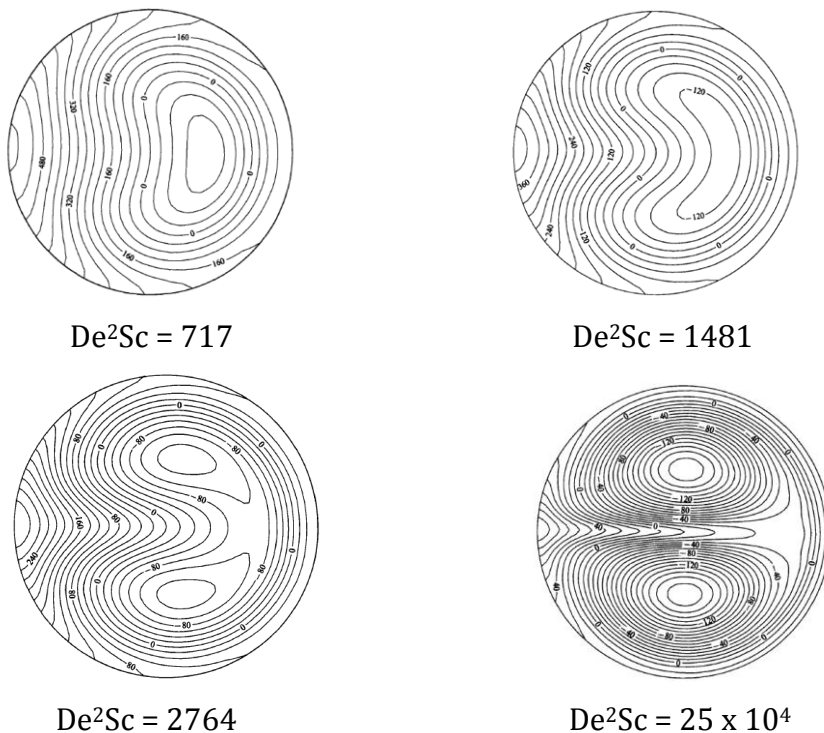


Figure 2.5. Dimensionless concentration profile of different values of parameter De^2Sc (figures from the publication by Johanson and Kamm⁷⁰).

2.3.Challenges of determining the diffusion coefficient by the Taylor dispersion analysis

Determination of the diffusion coefficient using the Taylor dispersion method requires taking into account several technical issues. First of all, the capillary has to be long enough to fulfill the conditions described in the previous chapters. Another issue is the rate of flow of the carrier phase. Most investigators apply low flow rates so that the value of De^2Sc is small and the impact of the centrifugal force on dispersion is negligible. For accurate measurements, velocity of the carrier should decrease with decreasing value of the diffusion coefficient. However, this significantly extends measurement time. Moreover, low flow rates are difficult to obtain in standard equipment used for this type of measurement. Therefore, diffusion coefficients determined using TDA for larger molecules may be questionable as large margin experimental errors are involved.

The above considerations indicate that in TDA application of high flow rates of the carrier phase would be most preferable. Therefore the aim of this thesis is to examine the dispersion process in a coiled capillary at high flow rates of the carrier phase.

The experimental part

3. Chemicals, equipment and procedures

3.1. Materials

Inorganic salts and buffers: potassium nitrate (KNO_3) and ortho-phosphoric acid (H_3PO_4) were from POCH (Gliwice, Poland). Alpha-tris-(hydroxymethyl)-methylamine (Tris) and phosphate buffered saline (PBS) was purchased from Sigma-Aldrich Chemie (Steinheim, Germany).

Peptides: Phe-Leu-Glu-Val, Val-Glu-Pro-Ile-Pro-Tyr, Tyr-Tyr-Tyr-Tyr-Tyr-Tyr, Val-Tyr-Val, Z-Phe-Leu, ZGly-Phe, Phe-Gly-Gly, Ala-Phe, Tyr-Ile-Gly-Ser-Arg, Gly-Leu-Tyr, and Gly-Gly-Tyr-Arg were purchased from Sigma-Aldrich Chemie (Steinheim, Germany).

Proteins: Ribonuclease A, apotransferrin, transferrin, lysozyme, beta-lactoglobulin, and insulin were purchased from Sigma-Aldrich Chemie (Steinheim, Germany).

Surfactants: sodium dodecyl sulfate (SDS) was purchased from Sigma-Aldrich Chemie (Steinheim, Germany).

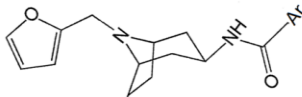
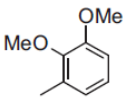
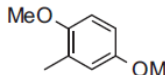
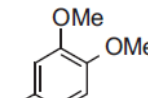
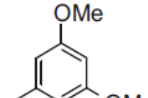
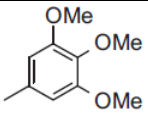
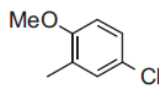
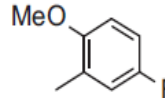
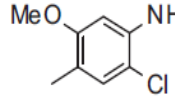
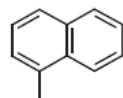
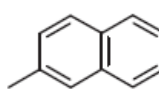
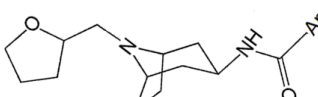
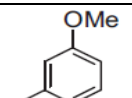
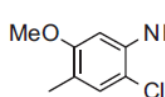
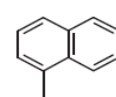
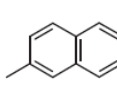
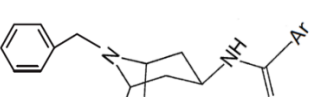
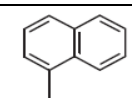
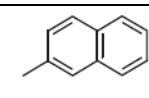
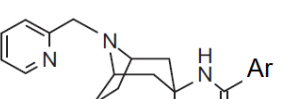
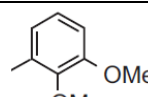
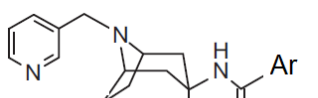
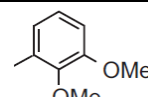
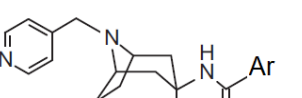
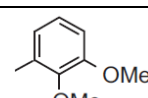
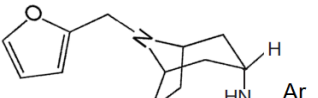
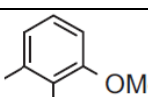
Bacteriophages: MS2, T4, λ were obtained at the Department of Molecular Biology at the University of Gdansk.

Drugs: warfarin, cefaclor, cefadroxil, diflunisal, etodolac, fenbufen, ibuprofen, imipramine and sulindac were purchased from Sigma-Aldrich Chemie (Steinheim, Germany).

Potential drugs: 3b- and 3a-aminotropane derivatives were synthesized at the Department of Drug Technology and Pharmaceutical Biotechnology at the Medical University of Warsaw. The structures of these compounds are shown in Table 3.1.

DNA hairpin: (Atto 488)- CGC AAA AAA AAA GCG- (Atto 647N) and (Atto 488)- CGC AAA AAA AAA GCG were purchased from FutureSynthesis Sp. z o.o.(Poland).

Table 3.1. Structures of the studied potential drugs (3b- and 3a-aminotropane derivatives).

Compound	Structure of the substituent Ar or R				
	 1	 2	 3	 4	 5
	 6	 7	 8	 9	 10
	 11	 12	 13	 14	
	 15	 16			
	 17				
	 18				
	 19				
	 20				

3.2. Sample preparation

All samples were prepared by dissolving a weighed amount of the studied compound in appropriate solvent, which was also used as a carrier phase. The following solvents were used:

TRIS buffer (pH = 7.4) for peptides, drugs and 3b- and 3a-aminotropane derivatives

PBS buffer (pH = 7.4) for proteins

TE buffer (pH = 8.0) for DNA hairpins

TRIS buffer with CsCl (4.5 M), MgSO₄ (10 mM) for bacteriophages

The mixtures were filtered through a filter with a nominal pore size of 0.22 µm to remove the suspended particles of the size over 0.22 µm.

3.3. Equipment

Experiments were conducted using equipment composed of:

- ✓ pump model LC-20AD Shimadzu (Kyoto, Japan) which can deliver flow rates from 0.0001 to 5 mL/min
- ✓ autosampler model SIL-20 AHT which makes it possible to introduce sample injection volumes from 0.1 µl to 100 µl
- ✓ PEEK (polyether ether ketone) capillaries with a 0.25 mm inner diameter (length 5, 10, 15, 30 m), 0.18 mm inner diameter (length 20 m), or 0.5 mm inner diameter (length 50 m) (Applied Research Europe GmbH, Germany)
- ✓ column oven model CTO-20AC which controls temperature range from 4 to 85°C (temperature control precision 0.1°C)
- ✓ UV-vis detector SPD-20A Shimadzu equipped with a flow cell of 10 mm path length and volume of 12 µl.
- ✓ PC computer using LC solution, version 1.25.
- ✓ degassing unit DGU-20A3R which removes gas bubbles from the carrier phase
- ✓ thermostat UTE-14 which keeps the temperature of the carrier phase constant

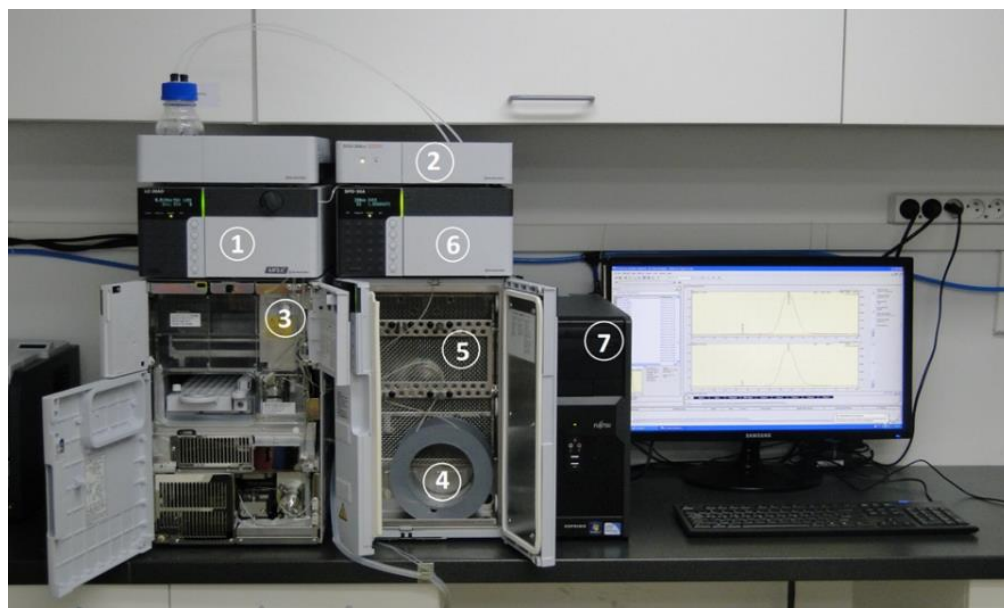


Fig. 3.1. Equipment which was used for Taylor dispersion experiments comprised 1- pump; 2 - degasser unit; 3 - autosampler; 4 - capillary; 5 - oven; 6 - UV-vis detector; 7 – computer

3.4. Determination of capillary radius

The average capillary radius was determined experimentally by measuring the time of filling a dry capillary with the carrier phase of known density. The obtained values of the radius of capillaries are presented in Table 3.2.

Table 3.2. The radiuses of capillaries determined experimentally.

L [m]	50	30	20	15	10	5
R [mm]	0.260	0.130	0.095	0.130	0.131	0.129

3.5. Experimental and calculation procedures

A small amount of liquid sample was injected into a carrier phase moving through a long, thin, coiled capillary. The narrow zone of the injected sample was dispersed in a capillary. Dispersion was the effect of action of convection and diffusion. The final concentration distribution of the studied compound was measured as absorbance in a function of time. The absorbance was measured at constant wavelength in the 12 μ l flow cell using UV-vis detector. The data were collected at

0.5s time step. Equation 2.27 and least square method were used to fit the data. The amplitude (A), the dispersion coefficient (σ), and the velocity (U) were the fitting parameters. The fitting procedure was carried out using the Microsoft Excel Office 2010 solver. In Figure 3.2. an example of fitting (Eq. 2.27) to the experimental data is shown.

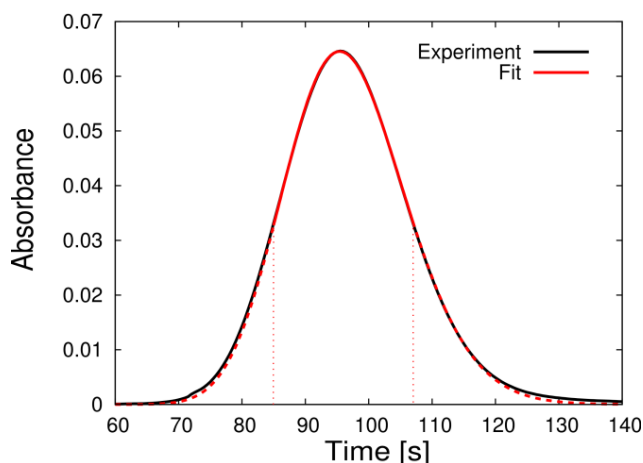


Figure 3.2. An example of concentration distribution obtained for L-phenylalanine using a 30 m long capillary at flow velocity $U = 31.5$ cm/s and fit (Eq. 2.27) to the experimental data (red line).

4. Results and discussion

Section 4.1. of this chapter presents measurements which were performed to validate the experimental method. In the next section, 4.2., a new approach to dispersion process in a coiled capillary is shown. Section 4.3. contains the results of diffusion coefficient measurements for various compounds and an attempt to determine the diffusion coefficient of bacteriophages. The final section 4.4. presents an application of the Taylor dispersion method for studying the denaturation process of proteins.

4.1. Validation of the experimental solutions

Many factors described in the literature part have to be considered in order to apply the Taylor dispersion method. Conditions 2.28, 2.30 and 2.31 were fulfilled by properly choosing of the dimensions of the capillary (a 30 m long capillary with

an inner diameter of 0.026 mm). Other factors which have an impact on these conditions are discussed in this section.

4.1.1. Flow rate

One of the most important parameters which we can control and change is the flow rate. In the experiments the flow rates in the range from 0.01 ml/min to 1 ml/min were used. This corresponds to linear velocity U in the range from 0.0032 m/s to 0.32 m/s for the inner diameter of the capillary 0.026 mm. Calculation of the Reynolds number allows to check whether the flow is laminar. In our case, for all velocities we used the flow was laminar. The values of the Reynolds numbers for selected velocities are shown in Table 4.1.

Table 4.1. The velocities and Reynolds numbers for the capillary dimension selected for the measurements reveal the laminar nature of the flow. Turbulent flows are expected for $Re > 2000$.

F [ml/min]	0.01	0.05	0.1	0.2	0.4	0.6	0.8	1
U [m/s]	0.0032	0.0158	0.0315	0.0630	0.1260	0.1890	0.2520	0.3151
Re	0.918	4.588	9.177	18.35	36.71	55.06	73.41	91.77

Flow velocity also has an impact on the secondary flow in a coiled capillary. According to literature, the parameter Dn^2Sc (Eqs 2.32 and 2.34) should be smaller than 20 to eliminate coiling effect.⁸ This criterion was checked experimentally by performing tests for the substance with a known diffusion coefficient (L-phenylalanine) at different velocities. Figure 4.1. shows dependence of the dispersion coefficient on the square of velocity. The experimental data are represented as solid red symbols. The values of dispersion coefficients calculated using the Taylor equation (Eq. 2.19) are also shown (black symbols).

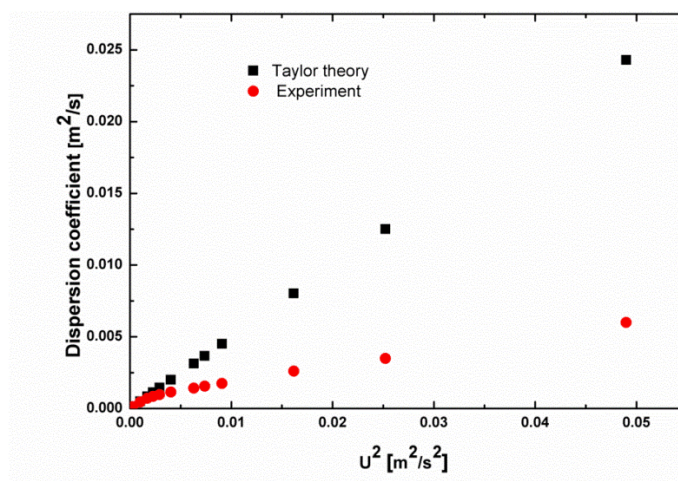


Figure 4.1. Dependence of the dispersion coefficient on the square of flow velocity determined for L-phenylalanine.

The results indicate that for $U > 0.0158$ m/s the impact of secondary flow on dispersion process becomes significant. This value of velocity corresponds to $Dn^2Sc = 43$, which differs slightly from the value reported in the literature ($Dn^2Sc = 20$). The values of parameter Dn^2Sc calculated for L-phenylalanine at other flow velocities are presented in Table 4.2.

Table 4.2. Values of parameter Dn^2Sc for L-phenylalanine at different velocities.

U [m/s]	0.0032	0.0158	0.0315	0.0630	0.1260	0.1890	0.2520	0.3151
Dn^2Sc	1.72	43.01	172.04	688.16	2752.63	6193.42	11010.53	17203.95

The value of the diffusion coefficient for L-phenylalanine obtained at $U = 0.0158$ m/s is 7.01×10^{-10} m²/s and is in a good agreement with the literature data obtained using a different method (7.10×10^{-10} m²/s).⁷¹ Application of such a low flow velocity causes elongation of the measurement time to even a few hours. Furthermore, the smaller is the diffusion coefficient, the lower flow velocity should be used to make the impact of the secondary flow negligible. In some cases it is impossible to use suitably low flow velocity due to technical limitations. Moreover, at low flow velocity the sample is much less dissolved by flow in comparison to higher flow velocities. Owing to this, in some cases (if the sample is too concentrated) we can observe dependence of the diffusion coefficient on concentration. In our case, despite the reduction in flow velocity, the error of

determination of the diffusion coefficient for proteins was 30-70 percent depending on the studied protein. For example the diffusion coefficient of lysozyme determined at $U = 0.0032$ m/s was 1.47×10^{-6} m²/s while the value given by literature was 1.1×10^{-6} m²/s. Similarly for apotransferrin, the experimental diffusion coefficient was 9.77×10^{-7} m²/s while in literature the diffusion coefficient was 5.7×10^{-7} m²/s. Thus it is possible to determine the diffusion coefficients for small molecules accurately at low flow velocity, but for large molecules the error is quite significant.

4.1.2. Injection volume

Numerical simulation made by Evans et al. (1965)⁵⁴ showed that the volume of the sample injected into the capillary should be much smaller in comparison to the volume of the capillary ($V_{inj}/V_{cap} < 0.01$). Due to this, the initial shape of the injected sample can be eliminated. Moreover, the sample has enough volume to disperse in the capillary (the signal is recorded when the concentration distribution is fully expanded).

In Figure 4.2. I show the dependence of the dispersion coefficient on the square of the velocity for different volumes of the injected sample (1 μ l, 5 μ l, 10 μ l, 50 μ l and 100 μ l). The measurements were carried out at different velocities of the carrier phase for L-phenylalanine. Figure 4.2. shows that the dispersion coefficients determined by injection of 1, 5 and 10 μ l of sample have similar values at all studied flow velocities. Deviations in dispersion coefficients were observed in the case of injection of 50 and 100 μ l of sample. It is connected with fact that condition 2.29 is not fulfilled for these injection volumes (see Table 4.3.).

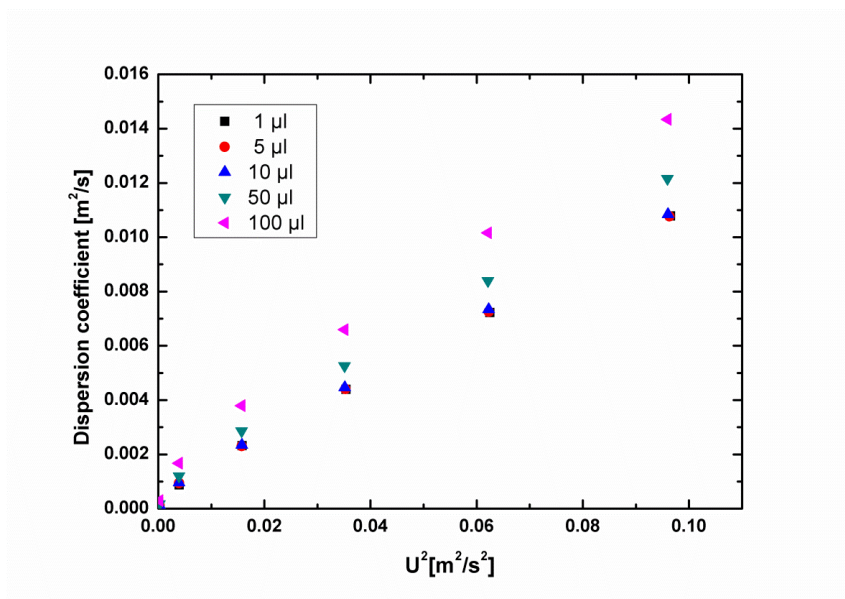


Figure 4.2. Comparison of relation of the dispersion coefficient to the square of the velocity for different injection volumes.

Table 4.3. Ratio of the injection volume to the capillary volume calculated for the applied injection volumes. Condition 2.29 is satisfied only for 1, 5 and 10 μl of samples. The volume of the capillary is 1.596 ml. The injection volumes 50 and 100 μl could be used only for capillaries of much larger volumes.

V_{inj} [μl]	$V_{\text{inj}}/V_{\text{cap}}$
1	0.001
5	0.003
10	0.006
50	0.031
100	0.063

4.1.3. Capillary length

Appropriate length of the capillary is essential for accurate measurements. Using a too short capillary results in the fact that the axial diffusion is not negligible and the ratio of the capillary volume to the injection volume is too large. In spite of this, the measurements using 15 m, 10 m and 5 m long capillaries were conducted to

analyze the changes of parameters affecting the dispersion coefficient. Different lengths of tubes were tested using L-phenylalanine as the injected substance for a wide range of flow velocities (0.0032-0.3151 m/s). The concentration distributions had the Gaussian shape for all capillary lengths. The dispersion coefficients were determined according to the procedure described earlier (see Section 3.5). The dispersion coefficient as a function of the flow velocity for various capillary lengths is presented in Figure 4.3. Although all data points form a Gaussian distribution, the location of the peak is not correct. With the decreasing lengths of the tube, the fitting velocity was incompatible with the value set on the pump (Table 4.4). It is probably connected with insufficient time necessary to obtain full mixing of the analyte (in the case of capillaries shorter than 30 m). In spite of this fact, random elimination of error occurs.

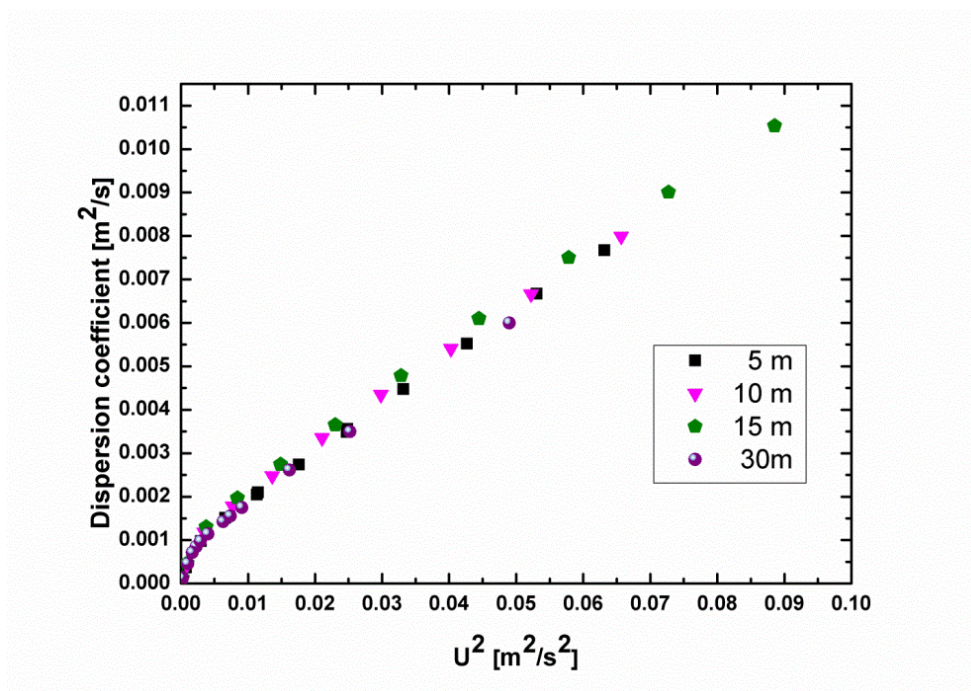


Figure 4.3. Dependence of the dispersion coefficient on the square of the velocity for different lengths of the capillary.

Table 4.4. Fitting flow velocity for measurement using different lengths of capillaries.

Set value of flow velocity [m/s]	Capillary length [m]			
	30	15	10	5
	Flow velocity determined from fitting [m/s]			
0.0158	0.0159	0.0155	0.0150	0.0138
0.0315	0.0321	0.0308	0.0295	0.0273
0.1575	0.1574	0.1521	0.1457	0.1320
0.3151	0.3110	0.2985	0.2825	0.2534

As presented in Table 4.4, for a 30 m long capillary the fitting velocity of flow is in agreement with the value set on the pump. For the capillary of length $L = 15$ m at high velocities we obtained deviations from a correct value. The deviations grew with the decrease in the length of the capillaries.

4.2. Analyzing dispersion process in a coiled capillary at high flow rates

The vortices which are generated at high flow rates in a coiled capillary make it impossible to use the Taylor equation (Eq. 2.19) for calculation of the diffusion coefficient (see Figure 4.1). The presence of vortices additionally mixes the analyte perpendicularly to the Poiseuille flow. As a consequence the analyte concentration distribution is narrower in comparison to the distribution in a straight capillary. A theoretical prediction made by Johanson and Kamm⁷⁰ shows that the width of the concentration distribution in a coiled capillary is reduced 5 times in comparison to the width of the concentration distribution for the same flow velocity but in a straight capillary. This section describes the experiments which disprove this prediction. A new solution for the dispersion process in a coiled capillary at high flow rates is presented.

4.2.1. A new solution for dispersion process in a coiled capillary at high flow rates

To check the Johanson and Kamm theory⁷⁰, the experiments for reference substances at high flow rates in a coiled capillary were performed. A 30 m long capillary with an inner radius of 0.13 mm and a coiling radius of 8 cm was chosen for measurements. As reference substances I used compounds of known diffusion coefficients: L-phenylalanine, warfarin, and apotransferrin (see Table 4.5.). The measurements were performed for a wide range of flow velocities (0.0158-0.315 m/s)

Table 4.5. Diffusion coefficients for three reference substances from literature data (D_{ref}).

Solute	$D_{\text{ref}} \times 10^{-10} \text{ (m}^2\text{s}^{-1}\text{)}$
L-phenylalanine	7.10 (ref 71)
Warfarin	4.90 (ref 72)
Apotransferrin	0.57 (ref 73)*

* value of the diffusion coefficient was calculated as described in Ref. 73 from the Stokes-Sutherland-Einstein equation.

The values of dispersion coefficients for these substances in a coiled capillary were determined according to the procedure described in Chapter 3. All concentration distributions had the Gaussian shape. Next, the theoretical dispersion coefficient (σ_s), which would appear if the capillary was straight, was calculated on the basis of the Taylor equation (2.19). The literature values of diffusion coefficients were taken for calculation. The parameter Dn^2Sc was calculated using Eqs 2.32 and 2.34 (for calculation of the Schmidt number I used the literature value of D). The density and viscosity of the carrier phase were the same as for water: $\rho = 997.044 \text{ kg/m}^3$, $\mu = 0.89 \times 10^{-3} \text{ Pa s}$ at 25 °C. Next, the ratio of the experimental dispersion coefficient (σ_c) in a coiled capillary to the theoretical dispersion coefficient (σ_s) in a straight capillary was plotted as a function of the parameter Dn^2Sc (see Figure 4.4.).

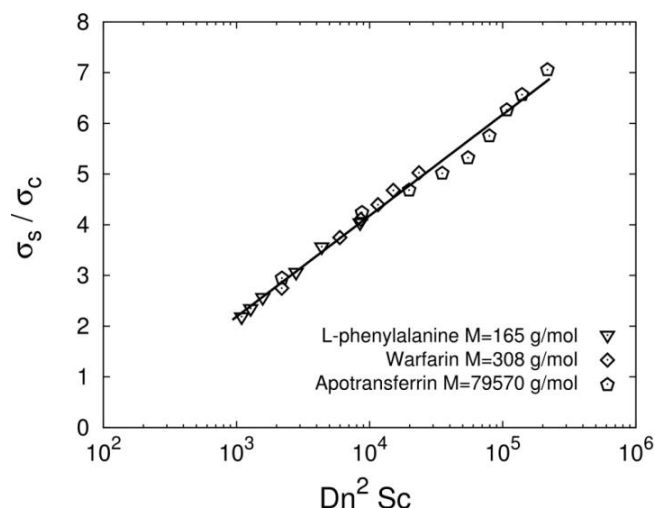


Figure 4.4. Dependence of the ratio of the dispersion coefficients in a straight capillary (σ_s) and in a curved capillary (σ_c) on the parameter Dn^2Sc , for three substances of known diffusion coefficient. Measurements were carried out using a 30 m long capillary with an inner radius of 0.13 mm and a coiling radius of 8 cm.

As predicted by Johanson and Kamm, the data fall onto a single curve, but the ratio of the dispersion coefficients in a straight capillary (σ_s) and in a curved capillary (σ_c) does not approach a constant value for $Dn^2Sc > 10^4$. In our case these data are well described by a logarithmic relation:

$$\frac{\sigma_s}{\sigma_c} = A \ln(Dn^2 Sc) + B \quad (4.1.)$$

where $A = 0.87 \pm 0.02$ and $B = -3.8 \pm 0.2$. A and B are two fitted parameters.

Solution of this equation for an unknown D is:

$$D = -\frac{1}{48} \frac{u^2 R^2}{\sigma_c A \cdot \text{Lambert W} \left(-1, -\frac{1}{192} \frac{r \mu e^{-\frac{B}{A}}}{R \rho \sigma_c A} \right)} \quad (4.2.)$$

The Lambert W function can be replaced with its asymptotic expansion:⁷⁴

$$\text{Lambert W}(-1, x) \approx W(x) = L_1 - L_2 + \frac{L_2}{L_1} + \frac{L_2(-2+L_2)}{2L_1^2}, \quad (4.3.)$$

where $L_1 = \ln(-x)$ and $L_2 = \ln(-\ln(-x))$

The impact of errors in various parameters on the sensitivity of equation 4.2. was tested. It was found that it is mainly the parameters A and B that influence the accuracy of measurements. The maximum errors calculated using differential analysis were in the range of 5-9%.⁷

4.2.2. Test of the equation

To check whether equation 4.2. works correctly for other substances, the dispersion coefficients in a coiled capillary at the velocity $U=31$ cm/s were determined for ribonuclease, lysozyme, and potassium nitrate. This equation was subsequently applied for calculation of diffusion coefficients. A very good agreement with literature data was obtained (see Table 4.6.).

Table 4.6. The diffusion coefficients calculated from equation 4.2. (D_{exp}) and literature data (D_{ref}). The error bars were calculated using differential analysis.*

Solute	$D_{\text{exp}} \times 10^{10} \text{ (m}^2\text{s}^{-1}\text{)}$	$D_{\text{ref}} \times 10^{10} \text{ (m}^2\text{s}^{-1}\text{)}$	$R_h \text{ (nm)}$
Lysozyme	1.26 ± 0.08	1.17 (ref 75)	1.95
Ribonuclease A	1.21 ± 0.08	1.21 (ref 76)	2.03
Potassium nitrate	17 ± 2.00	11.7-19.3 (ref 77)	0.15

The reference diffusivities D_{ref} were collected from the literature.

Additionally, the dispersion coefficients for these compounds at different velocities were determined. Then the σ , D_n , and S_c were calculated using formulas 2.32 and 2.34. These calculations used the previously determined value of the diffusion coefficient (D_{exp}). Next, the ratio of the experimental dispersion coefficient (σ_c) in a coiled capillary to the theoretical dispersion coefficient (σ) in a straight capillary, as a function of $D_n^2 S_c$ was plotted for these substances. In Figure 4.5. the data points for ribonuclease, lysozyme, and potassium nitrate are presented. This figure shows that the data points for these substances also fall onto the same curve. These results prove that equation 4.2. is correct.

* Differential analysis was made by dr Anna Ochab-Marcinek as a part of publication [78]

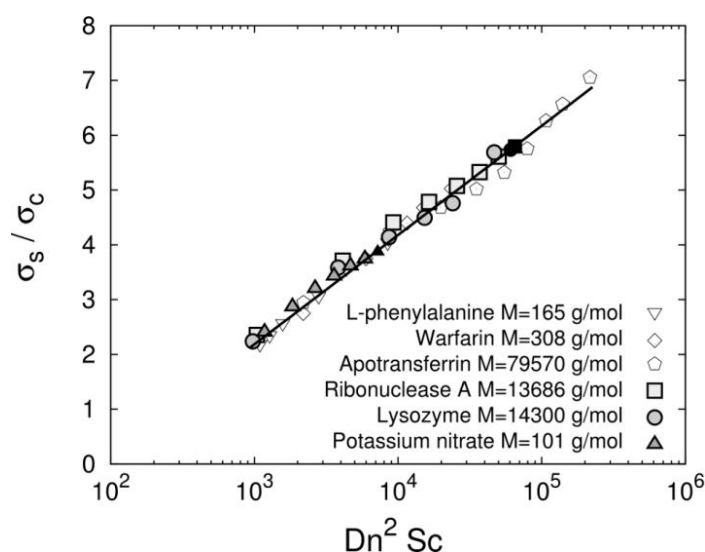


Figure 4.5. Dependence of the ratio of the dispersion coefficients in a straight capillary (σ_s) and in a curved capillary (σ_c) on the product of the Dean number squared and the Schmidt number for reference substances and for ribonuclease, lysozyme and potassium nitrate used as test compounds.

Afterward relation 4.1. was checked for different dimensions of the capillary and different flow velocities using reference substances: L-phenylalanine, warfarin and apotransferrin. The impact of the length and radius of the capillary and the radius of the capillary coiling were studied for the following combinations of capillary dimensions:

- ✓ Length of the capillary $L = 20$ m, radius of the capillary $R = 0.095$ mm, radius of the capillary coiling $r = 15$ cm
- ✓ Length of the capillary $L = 20$ m, radius of the capillary $R = 0.095$ mm, radius of the capillary coiling $r = 8$ cm
- ✓ Length of the capillary $L = 30$ m, radius of the capillary $R = 0.013$ mm, radius of the capillary coiling $r = 8$ cm
- ✓ Length of the capillary $L = 50$ m, radius of the capillary $R = 0.26$ mm, radius of the capillary coiling $r = 8$ cm

The ratio of the experimental dispersion coefficient (σ_c) in a coiled capillary to the theoretical dispersion coefficient (σ_s) in a straight capillary, as a function of Dn^2Sc was determined according to the procedure described earlier. The same

dependence was obtained for all the combinations of capillary dimensions (Figure 4.6.). These results indicate that equations 4.1. and 4.2. are correct for the range of the parameters studied in this investigation. This means that additional calibration is not necessary.

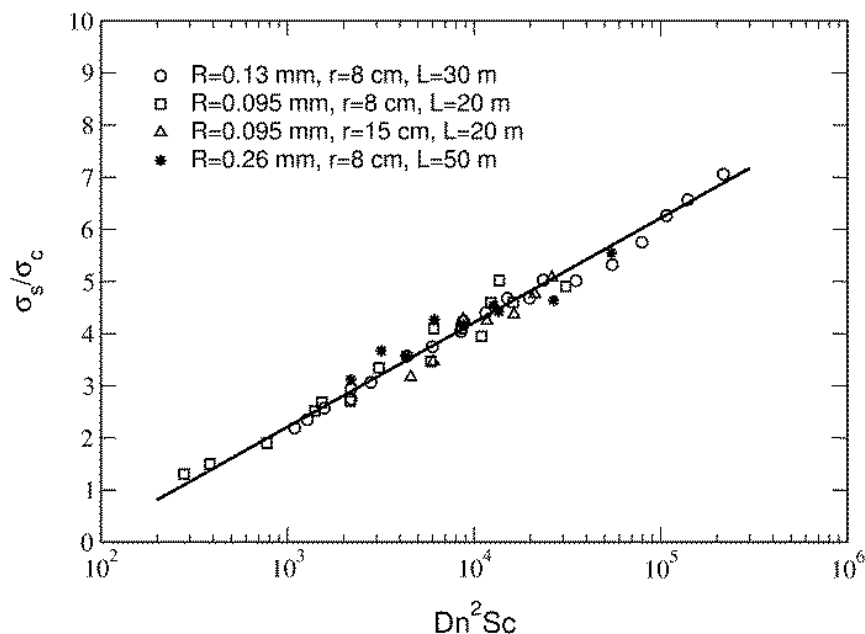


Figure 4.6. The dispersion coefficient in a straight capillary (σ_s) and in a curved capillary (σ_c) divided by the ones as a function of the product of the Dean number squared and the Schmidt number for different capillaries.

4.3. Application of a modified Taylor dispersion analysis for measurement of diffusion coefficients

In this section the results of diffusion coefficient measurements for peptides, drugs, potential drugs and DNA hairpins are presented. Additionally, an attempt to determine the diffusion coefficient of a few bacteriophages is shown. A 30 m long capillary with the inner radius of 0.13 mm and the coiling radius of 8 cm was used for measurements. Dispersion coefficient was determined according to the procedure described in Chapter 3. Subsequently, equation 4.2. presented in the previous section was applied for calculations.

4.3.1. Peptides

Peptides are compounds consisting of two or more amino acids linked by amide bonds. They have multiple applications in medicine and biotechnology as they play an important role in regulation of numerous physiological processes. They control and coordinate inter and intra-cellular communications and many of them play roles of hormones, cofactors, activators, stimulators or enzyme inhibitors. Their high selectivity, efficient activity, and low toxicity make them a focus of intensive studies on potential drugs.⁷⁹⁻⁸¹

The results of diffusion coefficient measurements for 11 peptides using TDA are presented in Table 4.7. Additionally, the hydrodynamic radii for these substances were calculated using measured values of diffusion coefficients and the Stokes–Sutherland–Einstein equation.

Table 4.7. Values of the diffusion coefficients and hydrodynamic radii of peptides.

Substance	M [g/mol]	$D_{\text{exp}} \times 10^{-10} \text{ (m}^2\text{s}^{-1}\text{)}$	$SD \times 10^{-13} \text{ (m}^2\text{s}^{-1}\text{)}$	$R_h \times 10^{-10} \text{ (m)}$
Ala-Phe	236.27	5.48	9.8	4.50
Phe-Gly-Gly	279.29	5.06	3.0	4.84
Gly-Leu-Tyr	351.4	4.48	3.3	5.45
Z-Gly-Phe*	356.37	4.58	29	5.34
Val-Tyr-Val	379.45	4.15	3.0	5.90
Z-Phe-Leu*	412.48	3.59	28	6.81
Gly-Gly-Tyr-Arg	451.48	3.96	2.3	6.18
Tyr-Ile-Gly-Ser-Arg	594.66	3.47	1.6	7.90
Phe-Leu-Glu-Glu-Val	635.71	3.22	3.2	7.59
Val-Gly-Pro-Ile-Tyr	716.82	3.04	2.2	8.04
Tyr-Tyr-Tyr-Tyr-Tyr-	997.05	1.68	44	14.6

* Z- carboxybenzyl group

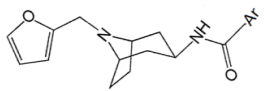
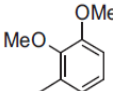
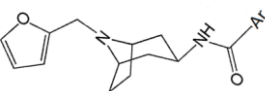
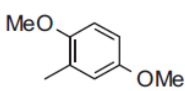
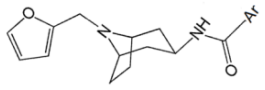
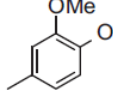

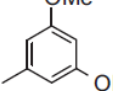
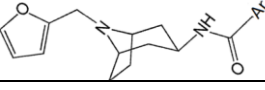
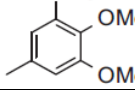

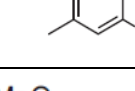

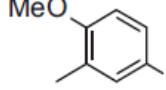

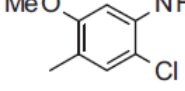

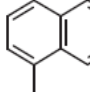
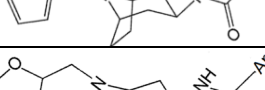
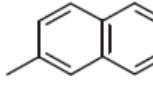
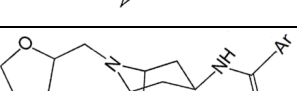
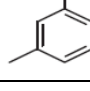

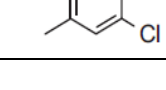
4.3.2. Drugs and potential drugs

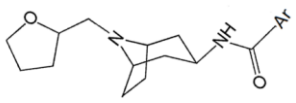
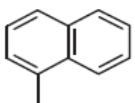
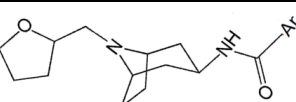
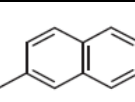
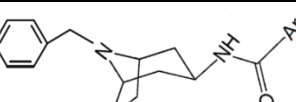
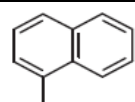
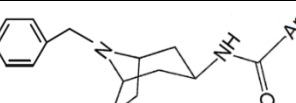
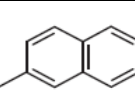
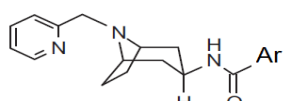
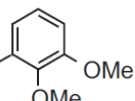
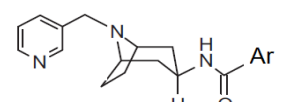
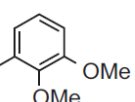
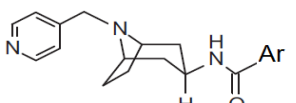
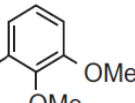
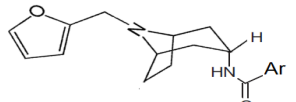
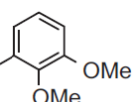
Knowledge of diffusion coefficients of drugs is essential to understanding the processes in which these drugs take part.^{71,82} There is a limited number of data concerning diffusivity of drugs in the literature. Therefore this thesis presents the experimentally determined diffusion coefficients for 10 well known drugs and for 20 potential drugs with potential antipsychotic activity. These potential drugs are 3b- and 3a-aminotropane derivatives synthesized in the Department of Drug Technology and Pharmaceutical Biotechnology at the Medical University of Warsaw. They are ligands of 5-HT_{1A}, 5-HT_{2A} and D₂ receptors and were obtained in the search for a new generation of antipsychotic drugs.

Table 4.8. Diffusion coefficients for drugs determined using the modified Taylor dispersion method.

Compound	$D_{\text{exp}} \times 10^{-10} (\text{m}^2\text{s}^{-1})$	$SD \times 10^{-12} (\text{m}^2\text{s}^{-1})$
Cefaclor	3.74	8.4
Cefadroxil	2.98	1.2
Desvenlafaxine hydrochloride	3.94	1.9
Diflunisal	5.27	4.1
Etodolac	4.06	4.7
Fenbufen	4.61	2.9
Ibuprofen	4.56	3.8
Sulindac	3.94	6.6
Tramadol hydrochloride	4.29	2.1
Venlafaxine hydrochloride	3.76	1.5

Table 4.9. Diffusion coefficients for 3b- and 3a-aminotropane derivatives (of potential antipsychotic activity) determined using modified Taylor dispersion method.

Compound No.	Compound	Ar	D x 10 ⁻¹⁰ (m ² s ⁻¹)	SD x 10 ⁻¹² (m ² s ⁻¹)
1.			4.35	1.7
2.			3.97	2.9
3.			3.97	1.2
4.			3.87	2.3
5.			3.80	1.7
6.			2.29	1.2
7.			4.07	1.2
8.			3.37	3.5
9.			3.17	5.2
10.			2.18	2.9
11.			3.97	1.7
12.			3.78	5.8

Compound No.	Compound	Ar	D x 10 ⁻¹⁰ (m ² s ⁻¹)	SD x 10 ⁻¹² (m ² s ⁻¹)
13.			4.17	1.2
14.			3.62	1.7
15.			2.04	1.2
16.			2.07	1.9
17.			3.94	1.7
18.			3.97	4.0
19.			3.97	4.6
20.			4.25	4.2

4.3.3. DNA hairpins

DNA hairpins are the structural elements of single-stranded DNA, which appear when two regions of the same strand of DNA containing the complementary bases in a correct sequence to those that appear earlier in the strand form a double helix. They play a key role in DNA recombination, DNA replication and regulation of gene transcription.⁸³⁻⁸⁶ DNA hairpins are not static, but fluctuate between close and open state. Kinetics of DNA hairpins was studied using i.a. NMR^{87,88} and fluorescence correlation spectroscopy FCS.⁸⁹⁻⁹¹

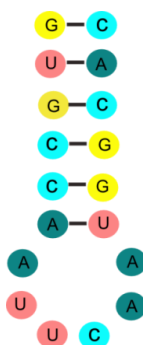


Figure 4.7. Schematic illustration of a DNA hairpin

In this section I present the results of determining the diffusion coefficient of two DNA hairpins with the following sequences:

1. (Atto 488)- CGC AAA AAA AAA GCG
2. (Atto 488)- CGC AAA AAA AAA GCG- (Atto 647N)

These DNA hairpins were synthetic. The first DNA hairpin was labeled with Atto 488 dye and the second was labeled with two dyes, Atto 488 and Atto 647. These DNA hairpins were dissolved in TE buffer (10 mM Tris/HCl, 1mM EDTA), which was also used as a carrier phase. The measurements were performed at flow rates of the carrier phase being in the range of 0.4-1 ml/min. The absorbance was measured at 260 nm.

Table 4.10. Comparison of the diffusion coefficients determined for both DNA hairpins at different flow rates. The diffusion coefficient slowly increases with the growing flow rate.

Flow velocity (m/s)	Diffusion coefficient of DNA hairpin (1) $\times 10^{-10}$ (m^2s^{-1})	SD $\times 10^{-12}$ (m^2s^{-1})	Diffusion coefficient of DNA hairpin (2) $\times 10^{-10}$ (m^2s^{-1})	SD $\times 10^{-12}$ (m^2s^{-1})
0.315	1.05	1.2	1.06	1.3
0.252	1.02	1.0	1.05	1.2
0.189	1.10	1.1	1.13	1.2
0.126	1.20	1.2	1.23	1.3

The obtained values of diffusion coefficients for both DNA hairpins at the same flow rate are very close to each other (see Table 4.10). However, slight dependence of diffusion coefficient on the flow velocity is observed for both DNA hairpins. The diffusion coefficient increases with decreasing flow velocity. This effect is probably related to fluctuations of the hairpins between the open and closed state. At lower flow velocities the hairpins have more time to create hydrogen bonds. This topic requires additional tests applying different methods.

4.3.4. Bacteriophages

Bacteriophages are viruses that infect specific bacteria. They destroy bacteria by multiplying within their cells and breaking them down. Bacteriophages consist of the following elements:

- ✓ nucleic acid (it can be either DNA or RNA but not both)
- ✓ a protein coat (capsid) which plays the role of a protective coverage of the nucleic acid

Many bacteriophages have additional elements:

- ✓ a tail which is a tube through which the nucleic acid passes when the bacteria is infected
- ✓ a base plate and tail fibers which are elements helping the phage to attach to the bacterial cell

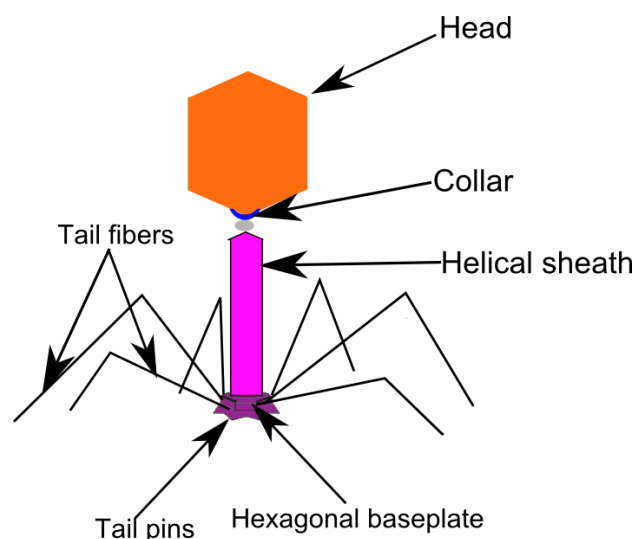


Figure 4.8. A typical structure of a tailed bacteriophage.

In this section I present a study of diffusivity for three bacteriophages: MS2, Lambda and T4, using Taylor dispersion method. These phages differ in structure and size.

Bacteriophage MS2

The MS2 belongs to *Leviviridae* family. It infects the bacterium *Escherichia coli* and other members of the *Enterobacteriaceae*. This phage is of small size (diameter = 28 nm) and has a simple structure. It consists of a single stranded RNA genome and an icosahedral capsid.⁹²

Bacteriophage lambda

Bacteriophage λ (*Siphoviridae* family) is composed of a double-stranded linear DNA, an icosahedral head with a diameter of 60 nm and a tail 150 nm long. It may also contain tail fibers. The tail's external diameter is 9-18 nanometers.⁹³

Bacteriophage T4

Bacteriophage T4 is a representative of the *Myoviridae* family. Like other viruses of this group it is characterized by double-stranded DNA genome, an extended icosahedral shrink head and a tail connected to the baseplate with long tail fibers. It is one of the largest phages, approximately 200 nm long and 80-100 nm wide including the capsid.⁹⁴

Description of the experiments

The bacteriophages were prepared at the Department of Molecular Biology at the University of Gdansk. The bacteriophages were kept in 10 mM Tris-HCl at pH 7.4, 4.5 M CsCl, 10 mM MgSO₄. Two different batches of bacteriophages were tested: the first contained bacteriophages prepared three weeks earlier and the second one was prepared 2 days before the experiment. The absorbance was measured at 260 nm for all samples and the injection volume was 10 μ l in all cases. The results for the first batch are presented in Figures 4.9, 4.10. and 4.11.

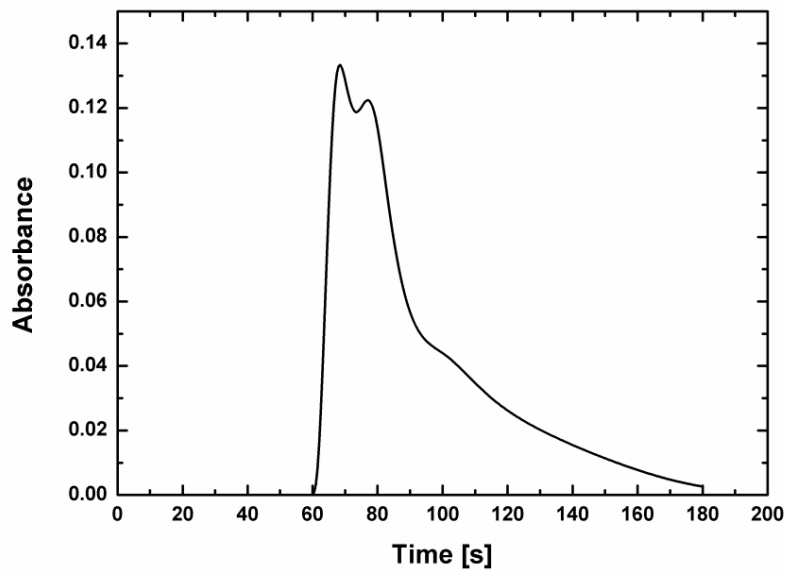


Figure 4.9. Concentration distribution obtained for λ bacteriophage from the first batch.

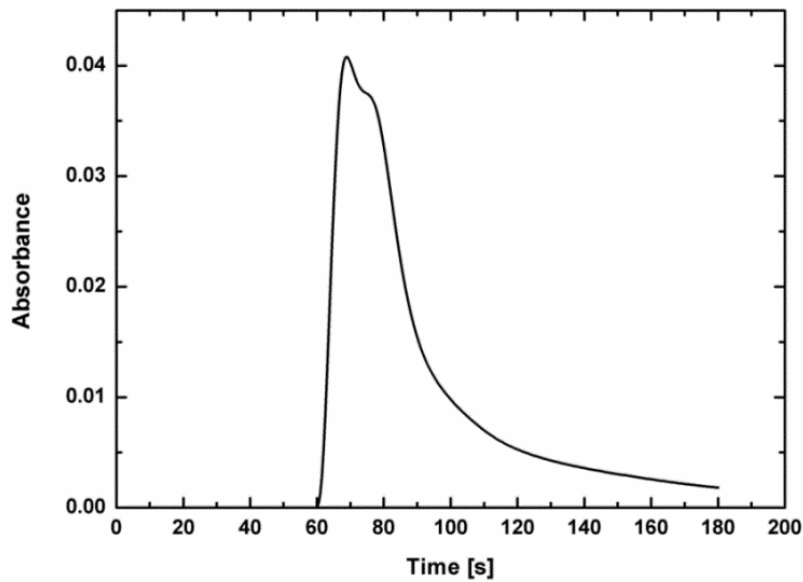


Figure 4.10. Concentration distribution obtained for MS2 bacteriophage from the first batch.

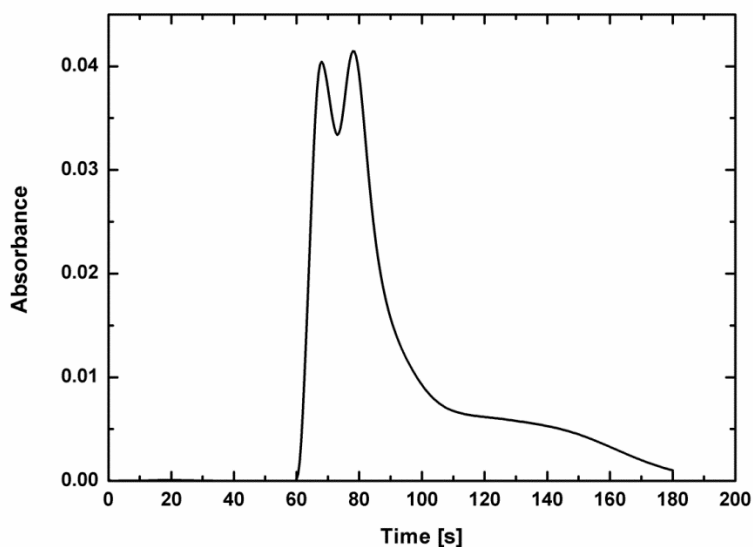


Figure 4.11. Concentration distribution obtained for T4 bacteriophage from the first batch.

The shapes of the concentration distribution obtained for all examined bacteriophages from the first batch are non-Gaussian and the presence of additional peaks is clearly visible. The results indicate presence of additional components in the samples. It is probably connected with degradation of bacteriophages or with initiation of DNA injection. The sample had most likely degraded during storage.

Therefore, the second batch was studied, freshly prepared two days before the measurements. Figures 4.12, 4.13. and 4.14 present the concentration distributions for the bacteriophages from the second batch. The obtained distribution curves for bacteriophages λ and MS2 are more symmetrical than the ones for the same bacteriophages from the first batch. Nevertheless, these distributions were not repetitive in subsequent injections and diffusion coefficients determined from these distributions differed significantly. The concentration distribution for bacteriophage T4 was, as previously, non-symmetrical.

These results confirmed that samples were not stable. Thus it was not possible to determine the correct value of diffusion coefficient in this case.

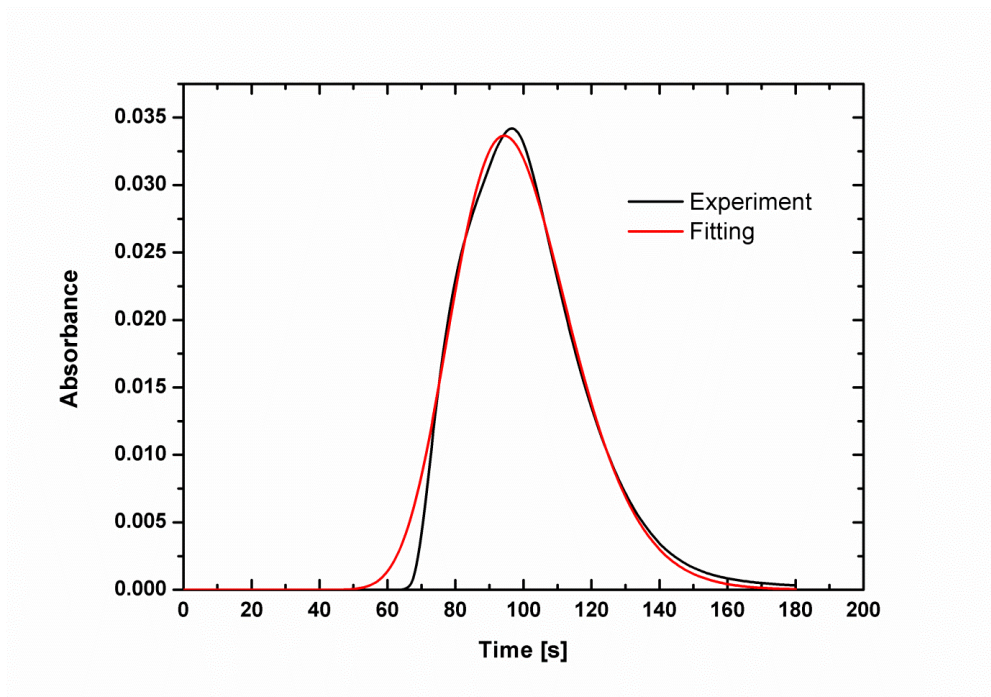


Figure 4.12. Concentration distribution obtained for λ bacteriophage from the second, freshly prepared batch.

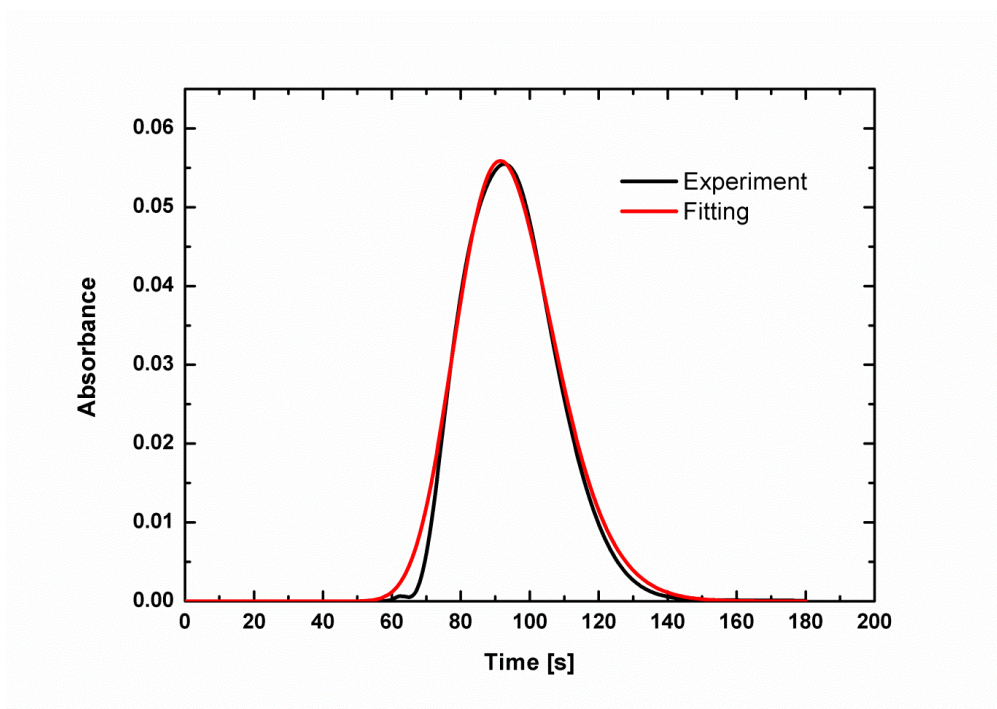


Figure 4.13. Concentration distribution obtained for MS2 bacteriophage from the second, freshly prepared batch.

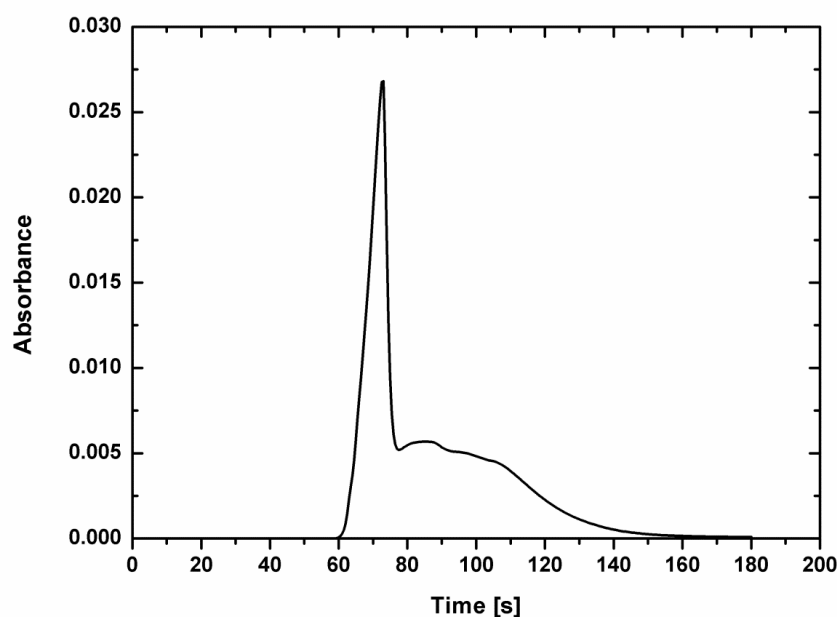


Figure 4.14. Concentration distribution obtained for T4 bacteriophage from the second, freshly prepared batch.

4.4. Study of denaturation process of proteins by surfactants

4.4.1. Introduction

Proteins are large biological macromolecules that are built from amino acids covalently bonded by peptide bonds. They can be composed of one or more polypeptide chains. The function of proteins depends on their structure, which can be described at four levels of complexity. The primary structure refers to the linear sequence of amino acids in a protein chain. The secondary structure describes areas of folding or coiling of the chain. The proteins can create two types of the secondary structure: the α -helix and the β -sheet. The tertiary structure is connected with three-dimensional shape of protein. It is held by the following types of interaction between side chain groups of amino acids: hydrogen bonding, ionic interactions of the positively and negatively charged groups, hydrophobic interactions, disulfide bridges and van der Waals forces. The quaternary structure concerns proteins which contain more than one polypeptide chain and describes the organization of protein subunits.^{95,96}

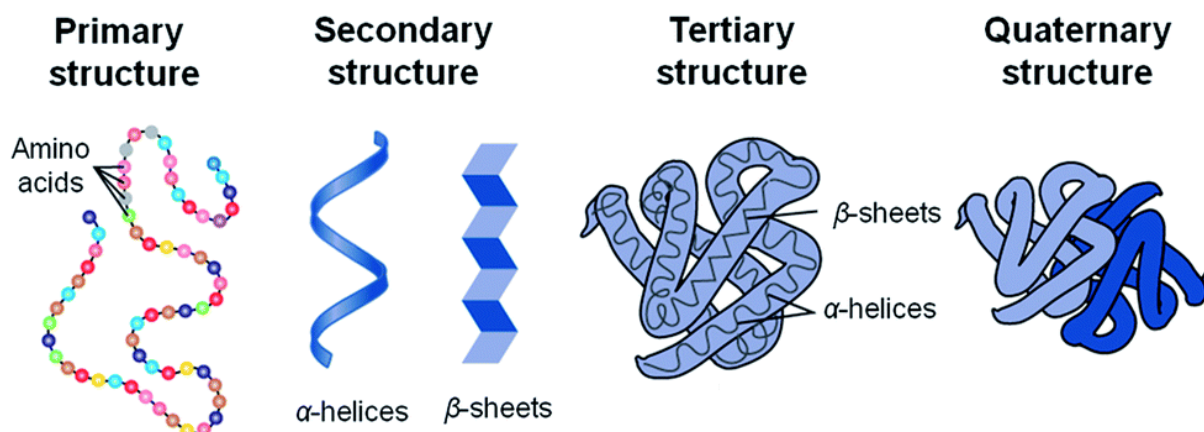


Figure 4.15. Different levels of protein structure (adapted from ref. 97).

Some changes in environment, such as addition of certain compounds,^{98,99} or increase in temperature,^{100,101} may cause protein denaturation i.e. alteration of the protein shape (generally unfolding). After denaturation most of proteins lose their biological functions. Moreover, a partially unfolded form of protein is often the precursor of aggregation of proteins. It leads to formation of a fibrous structure. Some fibrous structures, the so-called amyloid fibrils, are closely related to pathological changes in functioning of the organism.^{102,103}

One of the classes of compounds which can induce the unfolding of proteins are surfactants.¹⁰⁴⁻¹¹¹ These compounds are composed of both hydrophilic and hydrophobic groups. Surfactants are often classified with regard to the electrical charge of the hydrophilic part in water solution. According to this criterion they can be divided into four groups: anionic, cationic, amphoteric (where the molecules contain both positive and negative charges) and non-ionic.¹¹² Surfactants exist as solubilized monomers below concentration known as the critical micelle concentration (CMC). Above this concentration surfactant molecules aggregate and form so-called micelles, which coexist with the monomeric form of the surfactant. Increasing surfactant concentration above CMC causes formation of micelles while the concentration of the monomers remains nearly the same as at CMC (Figure 4.17.).¹¹¹

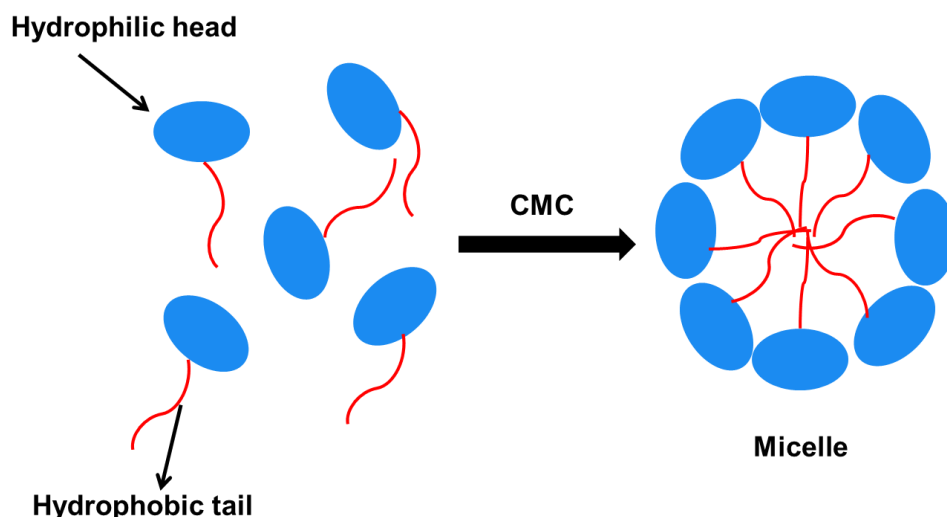


Figure 4.16. Schematic illustration of micelle formation.

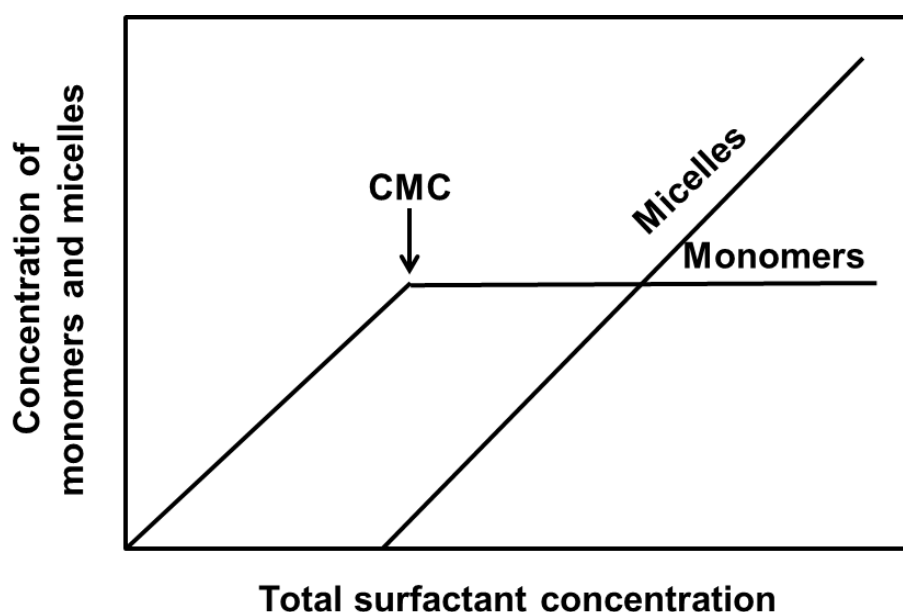


Figure 4.17. Schematic illustration of concentrations of monomer and micellar forms of surfactant. Micelles appear at the critical micelle concentration (CMC) and from this point concentration of micelles increases while concentration of monomers does not change and is equal to the CMC.

One of the parameters which can be used to characterize a micelle is the aggregation number. This number describes the number of monomers in a micelle. Typically micelles contain between 20 and 100 monomers¹¹³ and may have different shapes, i.e. spheres, rods or lamellae, depending on the surfactant

concentration. For example, for SDS the aggregation number is 55 at the concentration 20 mM and 64 at 50 mM.¹¹⁴ At these concentrations the micelles have ellipsoidal shape, but above 50 mM micelles undergo a transformation to a “rodlike” shape.¹¹⁵ Three types of forces are responsible for micelle formation: the hydrophobic repulsion between a hydrocarbon chain and water, the charge repulsion of the ionic part of the surfactant, and van der Waals attraction between the hydrophobic chains of the surfactant. Therefore, addition of electrolytes has an impact on micelle formation. The CMC decreases as the ionic strength increases.¹¹¹ The reason for such a strong effect of electrolyte additive is the reduction of electrostatic repulsion between the ionic headgroups.

The critical micelle concentration is essential for the understanding of the mechanism of interaction between surfactants and proteins (some proteins are denatured by surfactant monomers while others are denatured by micelles). Protein-surfactant interactions are often described by binding isotherms (Figure 4.18). The binding isotherm shows dependence of the average number of surfactant molecules bound per protein molecule (\bar{V}) on the logarithm of the free surfactant concentration. The isotherm of binding can be divided into four characteristic regions with increasing surfactant concentration. These regions correspond to different types of interactions. The first region (at the lowest surfactant concentration) is connected with a specific binding, which is predominantly electrostatic. In this region monomers of the surfactant bind to the oppositely charged groups on the protein. The second region is characterized by gradual binding of the surfactant molecules (non-cooperative interactions). Then the binding isotherm shows a dramatic increase in binding number because of cooperative interactions. Cooperative binding means that the binding affinity increases as more surfactant is bound. Next, saturation is observed: it means that all available binding sites are saturated with SDS and that normal micelle formation occurs as excess surfactant is added.¹¹⁶

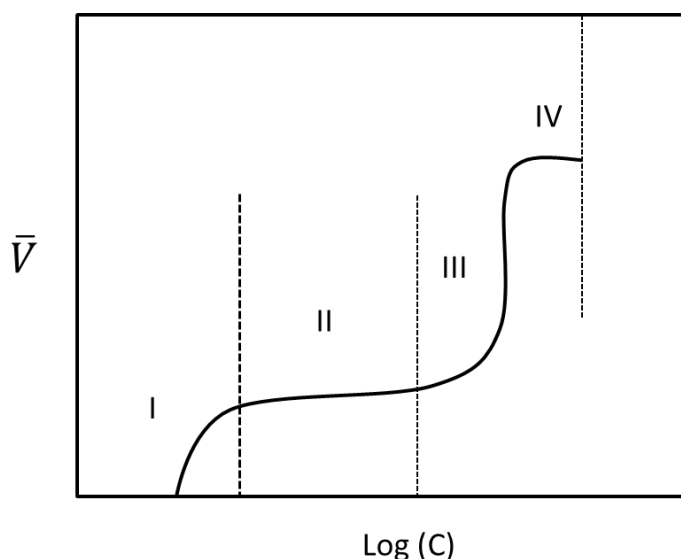


Figure 4.18. Schematic illustration of a binding isotherm.

4.4.2. Study of denaturation of proteins by surfactant using the Taylor dispersion method

Denaturation of transferrin, β -lactoglobulin and insulin by sodium dodecyl sulfate (SDS) was studied using the Taylor dispersion method. A series of measurements were performed at constant protein concentration and varying SDS concentrations. The concentration for transferrin was 1.9×10^{-5} M, for β -lactoglobulin was 7.6×10^{-5} M, and for insulin was 1.2×10^{-4} M. The concentration of SDS varied from 1.2×10^{-4} M to 8.7×10^{-2} M. Structural changes of the proteins were analyzed based on the diffusion coefficients of the complexes, which were formed at different surfactant concentrations. All experiments were conducted in PBS buffer (pH 7.4) at 25°C.

Figures 4.19, 4.20 and 4.21 show the diffusion coefficient of the protein-SDS complexes plotted as a function of the total surfactant concentration for the systems of transferrin-SDS, β -lactoglobulin-SDS and insulin-SDS respectively. These dependencies display two different regions (for all proteins) which may be compared with the cooperative binding region and saturation plateau region of the binding isotherm, while specific binding and non-cooperative binding regions are not visible due to too low sensitivity of the diffusion coefficient determination. This means that detectable increase of the diffusion coefficient is not observed. The critical surfactant concentration at which denaturation process starts was

determined based on the changes of the diffusion coefficient. Denaturation increases the size of a protein and consequently its diffusion coefficient decreases. The minimum concentration which induced structural changes was 4.3×10^{-4} M for transferrin and β -lactoglobulin and 2.3×10^{-4} M for insulin.

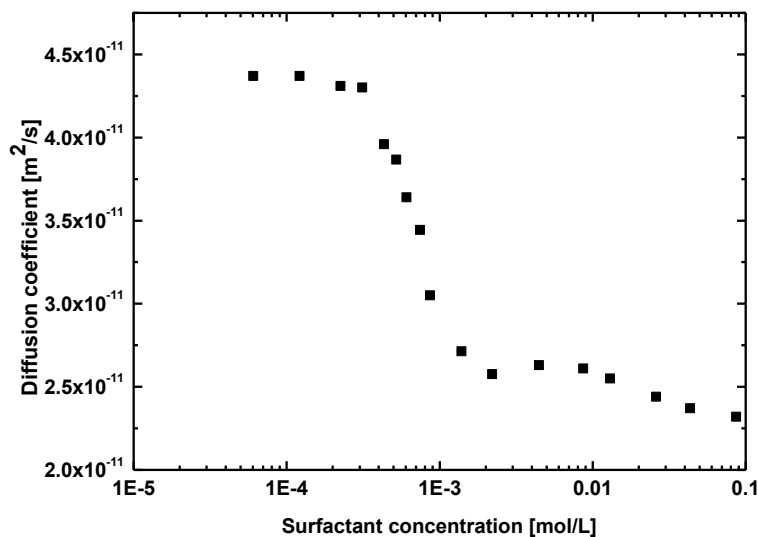


Figure 4.19. Dependence of the diffusion coefficient of transferrin on the surfactant concentration for transferrin-SDS system.

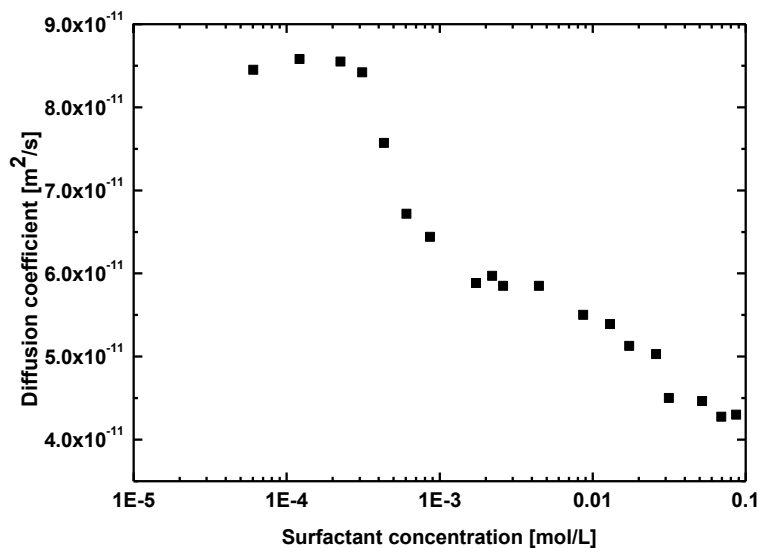


Figure 4.20. Dependence of the diffusion coefficient of β -lactoglobulin on the surfactant concentration for β -lactoglobulin-SDS system.

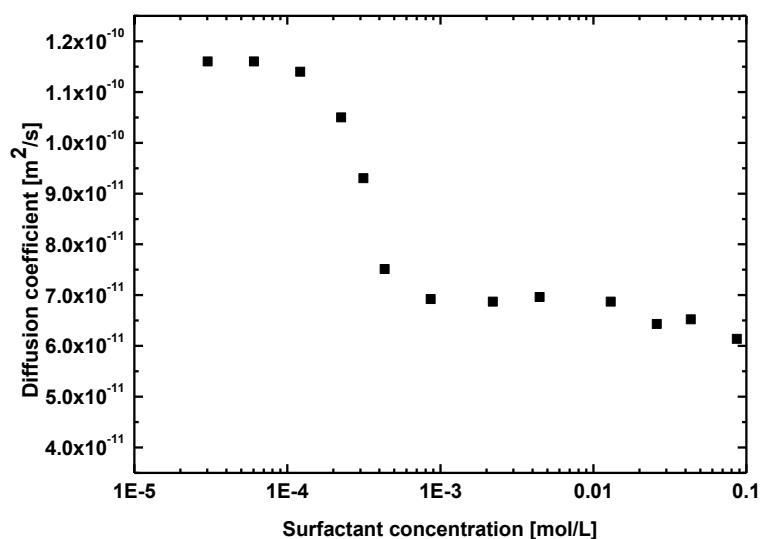


Figure 4.21. Dependence of the diffusion coefficient of insulin on the surfactant concentration for insulin-SDS system.

4.4.3. Circular dichroism measurements

The results obtained using the Taylor dispersion method were verified using circular dichroism (CD). Circular dichroism is a great tool for determining the tertiary structure of proteins. The CD spectrum of a protein in the 260-320 nm range provides information about aromatic amino acids. These amino acids give signals at characteristic wavelengths: phenylalanine in the region between 250-270 nm, tyrosine between 275 and 282 nm and tryptophan between 290-305 nm. In our studies CD was applied to study changes in the tertiary structure of transferrin, β -lactoglobulin and insulin under the influence of addition of sodium dodecyl sulfate (SDS).

The CD spectra for transferrin, β -lactoglobulin and insulin in PBS buffer with different amounts of SDS (0.016-25 mg/ml) were recorded using a Jasco J-815 spectropolarimeter in the 250-340 nm range. Measurements were performed at 25 °C. The solutions were measured in a quartz cell with the path length of 1 cm. The instrument was calibrated with buffer solution. All spectra were obtained using a scanning speed of 50 nm min⁻¹, a step size of 0.1, a bandwidth of 1 nm, a response time of 1 s, and an accumulation of 5 scans. The CD measurements were

performed in the cooperation with dr Marcin Górecki (Institute of Organic Chemistry PAS).

Analysis of structural changes in proteins

The CD spectra of transferrin, β -lactoglobulin, and insulin in buffer solution with different amount of sodium dodecyl sulfate (SDS) were shown in Figures 2.42, 2.43, and 2.44, respectively. The concentration of proteins was constant and for transferrin was 1.9×10^{-5} M, for β -lactoglobulin was 7.6×10^{-5} M, for insulin was 1.2×10^{-4} M. It was observed that when SDS is added to proteins, the ellipticity at 256 and 292 nm decreases with increasing the SDS concentration in the range of 2.1 - 6.9×10^{-4} M. When the concentration of SDS in solution reached 4.3×10^{-3} M for transferrin, the maximums and minimums in the spectrum disappeared. The observed change means that the tertiary structure of transferrin was destroyed. For β -lactoglobulin and insulin, addition of SDS at concentration 8.7×10^{-3} M lead to full destruction of the tertiary structure of these proteins.

The minimum concentration which induced structural changes was determined for all studied proteins. It was 4.3×10^{-4} M for transferrin and β -lactoglobulin and 2.3×10^{-4} M for insulin. The same minimum concentrations were determined using the Taylor dispersion method (see section 4.4.2). This is an evidence that the Taylor dispersion method works correctly.

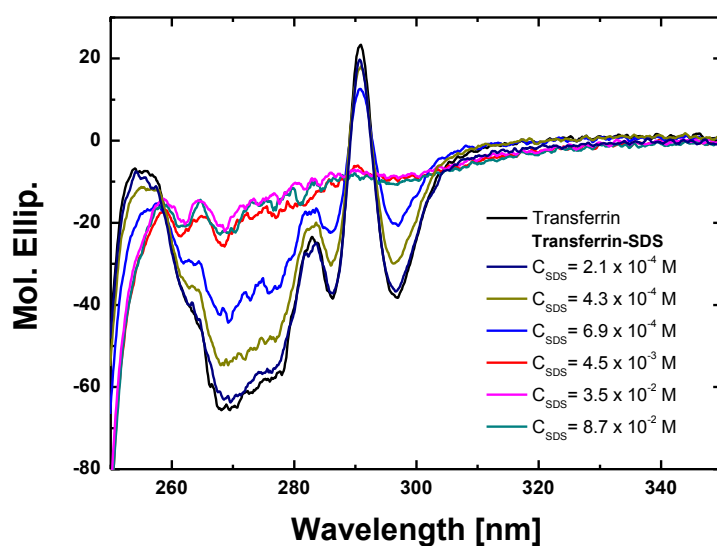


Figure 4.22. CD spectrum for transferrin in buffered solutions of sodium dodecyl sulfate (SDS).

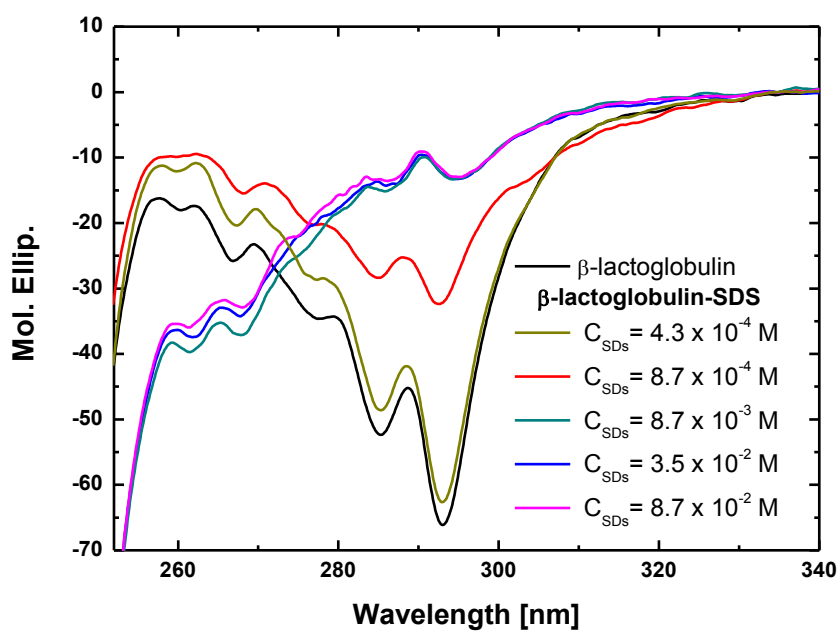


Figure 4.23. CD spectrum for β -lactoglobulin in buffered solutions of sodium dodecyl sulfate (SDS).

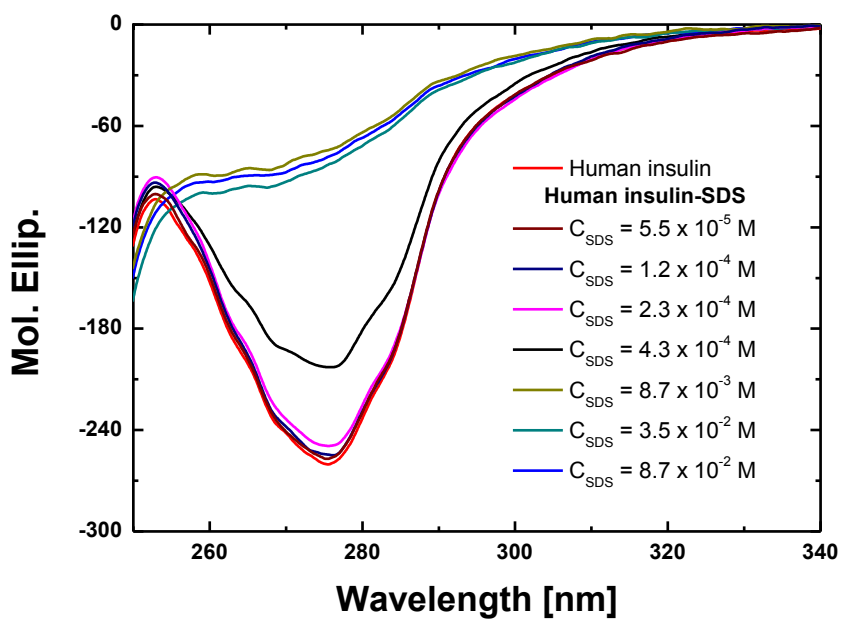


Figure 4.24. CD spectrum for human insulin in buffered solutions of sodium dodecyl sulfate (SDS).

4.4.4. Dynamic light scattering measurements

Dynamic light scattering was also applied to validate the Taylor dispersion method for studying protein denaturation. Structural changes of proteins, induced by addition of a surfactant, were analyzed based on the changes of the diffusion coefficient (as in TDA).

The measurements were performed using a Brookhaven BI-200SM goniometer equipped with Contin software. A stable argon ion laser with a wavelength of 514 nm was chosen for measurements. The intensity of scattered light was measured at several angles ranging from 30° to 150°. The diffusion coefficients were calculated as an average of the results determined at different scattering angles. The measurements were performed at 25°C. The samples were prepared in the same way as for TDA measurements. The SDS was dissolved in the PBS buffer, and then a small amount of this solution was used to prepare the protein-SDS buffer solution. Two types of sample were analyzed, one containing protein dissolved only in buffer solution, and the other one containing both protein and SDS dissolved in buffer. The concentration of SDS in these samples was 8.7×10^{-2} M. This concentration is much higher than critical micelle concentration (CMC) for SDS in PBS buffer; therefore we were sure that there were free micelles in solution. Owing to the fact that the intensity of autocorrelation functions were low (below 50%) for all studied systems, heterodyning effect could have significant impact on this function. Therefore we applied algorithm presented by Geissler which allowed us to remove a constant, uncorrelated signal from autocorrelation function.¹¹⁷

Analysis of structural changes in proteins

Figures 4.25, 4.26, and 4.27 show autocorrelation functions for the studied systems. For transferrin, experimental data were fitted using double exponential function. The concentration distributions showed two peaks for this system. One of them (at longer relaxation time) represents the relaxation of the transferrin-SDS complex and the other corresponds to the relaxation of the free SDS micelles. The diffusion coefficient changed from 4.54×10^{-11} m²/s for transferrin in buffer to 1.93×10^{-11} m²/s for transferrin-SDS complex. For β -lactoglobulin-SDS system autocorrelation function was fitted using double exponential function (similar to

transferrin-SDS system). The diffusion coefficient changed from $6.98 \times 10^{-11} \text{ m}^2/\text{s}$ for β -lactoglobulin in buffer to $4.20 \times 10^{-11} \text{ m}^2/\text{s}$ for β -lactoglobulin-SDS complex. However, the concentration distribution for insulin-SDS system showed only one peak in spite of the fact that in the solution there were two species: insulin-SDS complexes and free SDS micelles. It means that the relaxation times of these two species have similar values, indiscernible by DLS. In this case, it is impossible to determine the diffusion coefficients for them.

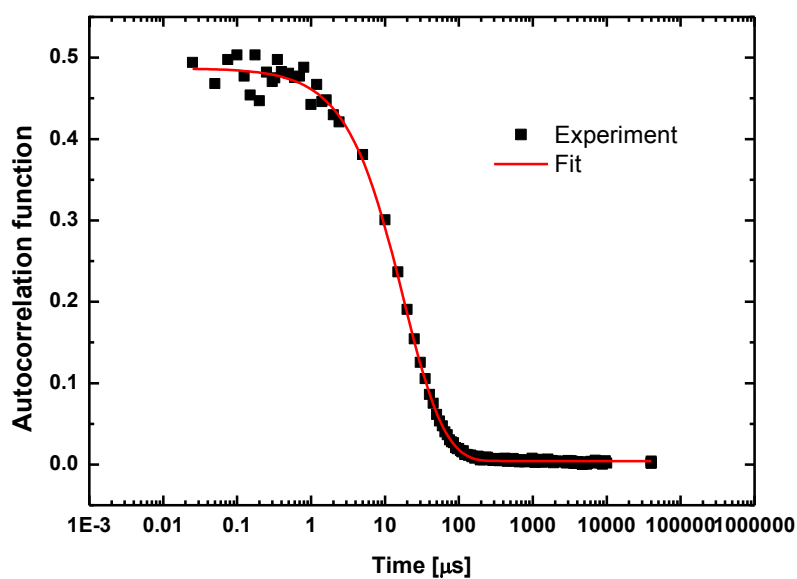


Figure 4.25. Autocorrelation function for transferrin-SDS system (the concentration of transferrin was $1.9 \times 10^{-5} \text{ M}$ and concentration of SDS was $8.7 \times 10^{-2} \text{ M}$) together with the exponential fit.

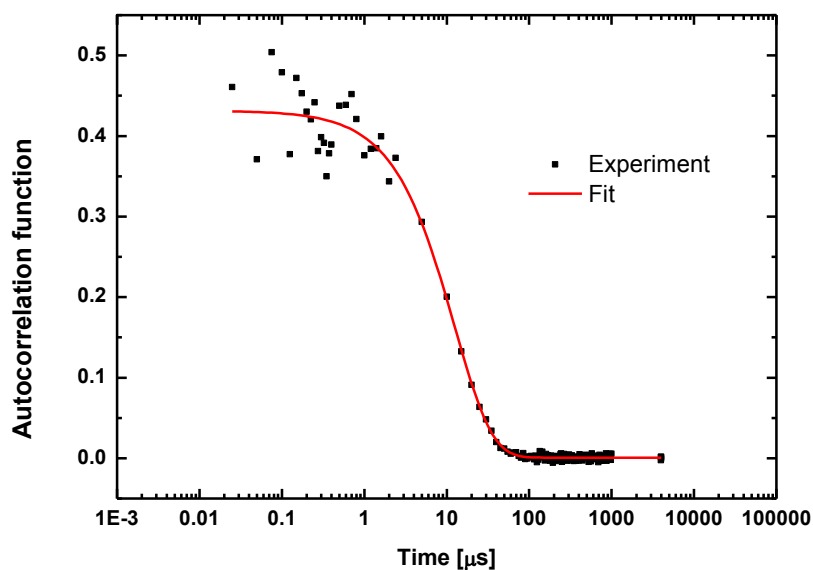


Figure 4.26. Autocorrelation function for β -lactoglobulin-SDS system (the concentration of β -lactoglobulin was 7.6×10^{-5} M and concentration of SDS was 8.7×10^{-2} M) together with the exponential fit.

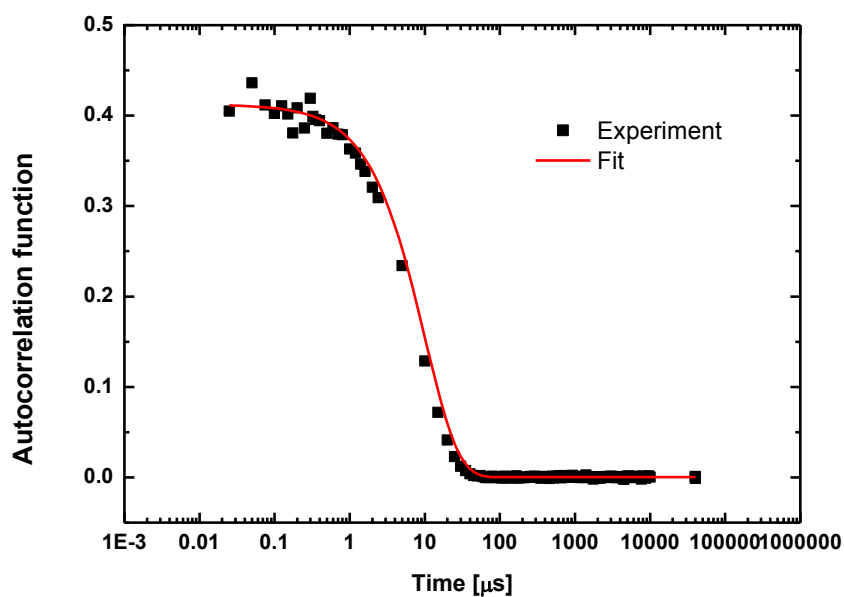


Figure 4.27. Autocorrelation function for human insulin-SDS system (the concentration of human insulin was 1.2×10^{-4} M and concentration of SDS was 8.7×10^{-2} M) together with the exponential fit.

Table 4.11. presents a comparison of diffusion coefficients determined using TDA and DLS for transferrin and β -lactoglobulin in PBS buffer and after adding SDS. The results obtained with both TDA and DLS show that the diffusion coefficient decreased approximately twice for the studied proteins after addition of SDS solution. It is another evidence that the Taylor dispersion method can be successfully applied to study protein denaturation.

However, the diffusion coefficient of β -lactoglobulin determined using DLS before addition of surfactant is lower than that obtained using TDA. The root of the problem is probably the presence of trace amounts of partially denaturated proteins in the sample. DLS is extremely sensitive to the presence of other objects of a similar size to the studied compounds (even at very low concentrations).

Table 4.11. Comparison of diffusion coefficients determined using TDA and DLS for transferrin and β -lactoglobulin in PBS buffer and after addition of SDS.

Protein	D (TDA) \pm SD \times 10^{-11} ($\text{m}^2 \text{s}^{-1}$)	D (DLS) \pm SD \times 10^{-11} ($\text{m}^2 \text{s}^{-1}$)	D (TDA) \pm SD \times 10^{-11} ($\text{m}^2 \text{s}^{-1}$)	D (DLS) \pm SD \times 10^{-11} ($\text{m}^2 \text{s}^{-1}$)
	Without addition of SDS		After structural transition	
Transferrin	4.37 \pm 0.01	4.54 \pm 0.06	2.16 \pm 0.08	1.93 \pm 0.06
β-lactoglobulin	8.14 \pm 0.01	6.98 \pm 0.05	4.29 \pm 0.01	4.20 \pm 0.22

5. Conclusions

Improvement of existing methods and solutions is an important element of technological progress in both industry and science. New approaches often eliminate or reduce certain technical restraints which held back progress in the past.

The main purpose of this study was to develop the Taylor dispersion method and create a simple, accurate and fast method for determining the diffusion coefficient. To achieve this goal, a detailed analysis of the dispersion process in a coiled capillary was performed. As a result, a scaling equation for the diffusion coefficient in a coiled capillary was determined. In a further part of this thesis, application of a modified Taylor dispersion method was presented. It was shown that this method can be used for determining the diffusion coefficient of peptides, proteins, drugs and DNA hairpins as well as being beneficial in the study of the denaturation of proteins by surfactants. Below I presented a summary, main conclusions and results contained in this thesis.

Section 4.1.

First of all, I analyzed the influence of different parameters such as velocity of the carrier phase, injection volume and capillary length on the quality of description of the experimental data. The most important conclusions from these studies were as follows:

- The vortices appear at flow velocity of the carrier phase higher than 0.016 m/s for a 30 m capillary with a diameter of 0.26 mm (for $Dn^2Sc > 43$)
- The length of the capillary is vital in the accuracy of measurement. It was observed that for a 15 m capillary and shorter the peak appears earlier - the earlier the shorter the capillary length - in comparison to the time which was expected from the flow velocity set on the pump
- The study of the impact of injection volume on the dispersion coefficient showed that the injection volume has to fulfill the condition 2.29.

These studies allowed us to select optimum parameter values (a 30 m long capillary with an inner diameter of 0.26 mm and 10 μ l of injected sample was selected for further measurements).

Section 4.2.

Next I performed experiments for reference substances at different flow velocities. It allowed me to determine the dependence of the ratio of the dispersion coefficient in a coiled capillary to the dispersion coefficient in a straight capillary on the product of the Dean number squared and the Schmidt number. The data was described by the relation 4.1. After that, equation 4.1. was solved for an unknown diffusion coefficient and as a result scaling equation 4.2. was obtained. Then the scaling equation was tested for different compounds, lengths, diameters, and curvatures of the capillary. The main conclusions of this part are as follows:

- The ratio of the dispersion coefficient in a coiled capillary to the dispersion coefficient in a straight capillary is a function of the parameter Dn^2Sc and is described by logarithmic relation 4.1.
- Additional studies for different lengths, diameters, and curvatures of the capillary showed that relation 4.1. is correct and is satisfied for all the tested capillaries.
- An unknown diffusion coefficient is determined from scaling equation (Eq. 4.2) supplemented by the experimental value of the dispersion coefficient.

Section 4.3.

The next part of this thesis concerned applying a modified Taylor dispersion method for determining the diffusion coefficients of compounds from different classes. Based on the results of this study I concluded that:

- The modified Taylor dispersion method can be successfully applied for studying the diffusion coefficients of both small (drugs) and large molecules (proteins).
- The Taylor dispersion method can be applied for studying the diffusion coefficients of bacteriophages but on condition that additional purification of the sample is applied.

Section 4.4.

In the last part of the experimental results, denaturation of proteins by surfactant using the Taylor dispersion method was shown. Conclusions from these studies are as follows:

- The dependence of the diffusion coefficient on surfactant concentration for all studied systems was observed. The changes in diffusion coefficient with increasing surfactant concentration indicated a gradual unfolding of proteins under the influence of the surfactant.
- Circular dichroism measurements were in accordance with the results obtained by the Taylor dispersion method. Determined minimum concentration which induces denaturation of proteins is the same as the one obtained using TDA.
- The size of the proteins at the highest surfactant concentration obtained by using the Taylor dispersion method is close to the size obtained using dynamic light scattering.
- The Taylor dispersion method can be used as a fast method for studying the denaturation of proteins.

To conclude, the development of the Taylor dispersion method made the method easy, fast, accurate and precise. It is a method complementary to such existing techniques as dynamic light scattering, diaphragm cell, fluorescence correlation spectroscopy and nuclear magnetic resonance. This method requires smaller volumes of samples and concentrations than diaphragm cell or dynamic light scattering and in addition is more precise and accurate than diaphragm cell or fluorescence correlation spectroscopy. In fact, TDA can be used for calibrating the fluorescence correlation spectrometer. This method is also very fast: determination of diffusion coefficient takes less than three minutes. Interpretation of the results is easier than in the case of other methods, and the low cost of the equipment is a big advantage. Chromatographic equipment in which a chromatographic column is replaced by a polymer capillary can be used for this type of measurements.

6. References

1. Cussler, E.L. *Diffusion: Mass Transfer in Fluid Systems*, Cambridge (2009).
2. Graham, T. H. On the law of diffusion of gases, *Phyl. Mag.* **2**, 175–191, 269–276, 351 – 358 (1833).
3. Graham T. On the motion of gases, *Phil. Trans.* **14**, 805 (1850).
4. Fick, A. On liquid diffusion, *Phyl. Mag.* **10**, 30–39 (1855).
5. Faghri, A., Zhang, Y., Howell, J. R. *Advanced Heat and Mass Transfer*, Global Digital Press (2010).
6. Burmeister, L. C. *Convective Heat Transfer*, John Wiley & Sons (1993).
7. Bejan, A., Kraus, A. D. *Heat Transfer Handbook*, John Wiley & Sons (2003).
8. Alizadeh, A., Nieto de Castro, C. A., Wakeham, W. A. The theory of the Taylor dispersion technique for liquid diffusivity measurements, *Int. J. Thermophys.* **1**, 243-284 (1980).
9. Bird, R.B., Stewart, W. E., Lightfoot, E. N. *Transport Phenomena*, John Wiley & Sons (2007).
10. Amidon, G. L., Lee, P. I., Topp, E. M. *Transport Processes in Pharmaceutical Systems*, Marcel Dekker, (2000).
11. Sinko, P. J. *Martin's Physical Pharmacy and Pharmaceutical Sciences*, Lippincott, (2009).
12. Berg, O. G., Vonhippel, P. H. Diffusion-controlled Macromolecular Interactions. *Annu. Rev. Biophys. Biophys. Chem.* **14**, 131–160 (1985).
13. Valeur, B., Berberan-Santos, M. N. *Molecular Fluorescence: Principles and Applications*, John Wiley & Sons (2013)
14. Sutherland, W. A dynamical theory of diffusion for non-electrolites and the mollecular mass of albumin, *Phil. Mag.* **9**, 781–785 (1905).
15. Einstein, A. On the motion of small particles suspended in a stationary liquid, as required by the molecular kinetic theory of heat, *Annalen der Physik*, **17**, 549 (1905).
16. Edward, J. Molecular volumes and Stokes-Einstein equation, *J. Chem. Educ.* **47**, 261–270 (1970).
17. Barnes, C., Measurements of diffusion coefficients by diaphragm cell method, *J. Appl. Phys.* **5**, 4 (1934).

18. Stokes, R. H. An improved diaphragm-cell for diffusion studies and some tests of the method, *J. Am. Chem. Soc.* **72**, 763–767 (1950).
19. Robinson, R. A., Stokes, R. H., *Electrolyte Solutions*, Butterworth, London, UK, 1960.
20. Robinson, R. L., Edmister, W. G., Dullien, F. A. L., Calculation of diffusion coefficients from diaphragm cell diffusion data, *J. Phys. Chem.*, **69**, 258 (1965).
21. Burns, N. L., Clunie, J. C., Baird, J. K. Diaphragm cell determination of the interdiffusion coefficients for aqueous solutions of copper sulfate, cobalt sulfate, and nickel sulfamate, *J. Phys. Chem.* **95**, 3801–3804 (1991).
22. Tropea, C., Yarin, A. L., Foss, J. F. *Springer Handbook of Experimental Fluid Mechanics*, Springer Science & Business Media (2007).
23. Annunziata, O., Buzatu, D., Albright, J. G. Protein diffusion coefficients determined by macroscopic-gradient Rayleigh interferometry and dynamic light scattering. *Langmuir*, **21**, 12085-12089 (2005).
24. Hawe, A., Hulse, W. L., Jiskoot, W., Forbes, R. T. Taylor Dispersion Analysis Compared to Dynamic Light Scattering for the Size Analysis of Therapeutic Peptides and Proteins and Their Aggregates, *Pharm. Res.*, **28**, 2302-2310 (2011).
25. Hou, S., Wieczorek, S., Kaminski, T. S, Ziebac, N., Tabaka, M, Sorto, N., Foss, M. H., Shaw, J. T., Thanbichler, M., Weibel, D. B., Nieznanski, K., Holyst, R., Garstecki, P. Characterization of *Caulobacter crescentus* FtsZ protein using dynamic light scattering. *J. Biol. Chem.* **287**, 23878–23886 (2012).
26. Schärftl, W. *Light scattering from polymer solutions and nanoparticle dispersions*, Springer (2007).
27. Uversky, V. N., Anatol'evich Permiākov, E. *Methods in Protein Structure and Stability Analysis: Conformational stability, size, shape, and surface of protein molecules*, Nova Publishers (2007).
28. Kissa E. *Dispersions: Characterization, Testing, and Measurement*, Marcel Dekker (1999).
29. Berne, B. J., Pecora, R. *Dynamic Light Scattering*, John Wiley & Sons (1976).
30. Pecora, R. *Dynamic Light Scattering: Applications of Photon Correlation Spectroscopy*, Springer (2013).

31. Enderlein, J., Gregor, I., Patra, D., Dertinger, T., and Kaupp, U. Performance of fluorescence correlation spectroscopy for measuring diffusion and concentration, *ChemPhysChem* **6**, 2324–2336 (2005).
32. Gendron, P.-O., Avaltroni, F., Wilkinson, K. J. Diffusion Coefficients of Several Rhodamine Derivatives as Determined by Pulsed Field Gradient-Nuclear Magnetic Resonance and Fluorescence Correlation Spectroscopy, *J. Fluoresc.* **18**, 1093–1101 (2008).
33. Lakowicz, J. R. *Principles of Fluorescence Spectroscopy*, Springer, Baltimore,(2006).
34. Krichevsky, O., Bonnet, G. Fluorescence correlation spectroscopy: the technique and its applications, *Rep. Prog. Phys.*, **65**, 251-297 (2002).
35. Lakowicz, J. R. *Topics in fluorescence spectroscopy*, volume 1. Kluwer Academic/ Plenum Publishers, (1999).
36. Stejskal, E. O., Tanner J. E. Spin diffusion measurements: spin echoes in the presence of a time-dependent field gradient, *J. Chem. Phys.* **42**, 288–292 (1965).
37. Noda, A., Hayamizu, K., Watanabe, M. Pulsed-gradient spin-echo ¹H and ¹⁹F NMR ionic diffusion coefficient, viscosity, and ionic conductivity of non-chloroaluminate room-temperature ionic liquids, *J. Phys. Chem.* **105**, 4603–4610 (2001).
38. Komlosh, M. E., Callaghan, P. T. Spin diffusion in semidilute random coil polymers studied by pulsed gradient spin-echo NMR, *Macromol.* **33**, 6824–6827 (2000).
39. Matsukawa, S., Ando, I. Study of self-diffusion of molecules in a polymer gel by pulsed-gradient spin-echo ¹H NMR. 2. Intermolecular hydrogen-bond interaction between the probe polymer and network polymer in N, N-dimethylacrylamide-acrylic acid copolymer gel systems, *Macromol.* **30**, 8310–8313 (1997).
40. Lapham, J., Rife, J. P., Moore, P. B., Crothers, D. M. Measurement of diffusion constants for nucleic acids by NMR, *J. Biomol. NMR J-Bio NMR* **10**, 255–262 (1997).
41. Heisel, K. A., Goto, J. J., Krishnan, V. V. NMR Chromatography: Molecular Diffusion in the Presence of Pulsed Field Gradients in Analytical Chemistry

- Applications, *Am. J. Anal. Chem.* **3**, 401–409 (2012).
42. Callaghan, P. T., *Principles of Nuclear Magnetic Resonance*, Oxford University Press, (1991)
43. Kimmich, R. *NMR: Tomography, Diffusometry, Relaxometry*, Springer, (1997).
44. Slichter, C. P., *Principles of Magnetic Resonance*, Springer (1978).
45. Cohen, Y., Avram, L., Frish, L. Diffusion NMR Spectroscopy in Supramolecular and Combinatorial Chemistry: An Old Parameter—New Insights, *Angew. Chem. Int. Ed.* **44**, 520 – 554 (2005).
46. Griffiths, A. On the movement of a coloured index along a capillary tube, and its application to the measurements of the circulation of water in a closed circuit, *Proc. Phys. Soc. London* **23**, 190 (1911).
47. Taylor, G. I. Dispersion of soluble matter in solvent flowing slowly through a pipe, *Proc. R. Soc. London, Ser. A*, **219**, 186-203 (1953).
48. Taylor, G. The dispersion of matter in turbulent flow through a pipe, *Proc. R. Soc. London, Ser A*, **225**, 473-477 (1954).
49. Probstein, R. F. *Physicochemical Hydrodynamics: An Introduction*, John Wiley & Sons (1994).
50. Nguyen N.-T. *Micromixers: Fundamentals, Design and Fabrication*, William Andrew (2011).
51. Aris, R. On the dispersion of a solute in a fluid flowing through a tube, *Proc. R. Soc. Lond. A*, **235**, 67-77 (1956).
52. Alizadeh, A. A., Wakeham, W. A. Mutual Diffusion Coefficients for Binary Mixtures of Normal Alkanes, *Int. J. Thermophys.*, **3**, 307-323 (1982).
53. Bielejewska, A.; Bylina, A.; Duszczyk, K.; Fialkowski, M.; Holyst, R. Evaluation of Ligand-Selector Interaction from Effective Diffusion Coefficient, *Anal. Chem.*, **82**, 5463–5469 (2010).
54. Evans, E. V., Kenney, C. Gaseous Dispersion in Laminar Flow Through a Circular Tube, *Proc. Roy.Soc.* **284**, 540-550 (1965).
55. Morrison, F. A. *An Introduction to Fluid Mechanics*, Cambridge University Press (2013).
56. Kundu, P. K., Cohen, I. M., Dowling, D. R. *Fluid Mechanics*, Academic Press (2012).

57. Dean, W. R. Note on the motion of fluid in a curved pipe. *Phil.Mag.* **4**, 208–223 (1927).
58. Dean, W. R. The stream-line motion of fluid in a curved pipe. *Phil.Mag.* **5**, 671–695 (1928).
59. Cheremisinoff, N. P. *Advances in Engineering Fluid Mechanics: Multiphase Reactor and Polymerization System Hydrodynamics*, Gulf Professional Publishing (1996).
60. Formaggia, L., Quarteroni, A., Veneziani, A. *Cardiovascular Mathematics: Modeling and simulation of the circulatory system*, Springer (2009).
61. White, C. M. Streamline flow through curved pipes, *Proc. Roy. Soc.* **123**, 645–663 (1929).
62. Taylor, G. I. The criterion for turbulence in curved pipes, *Proc. Roy. Soc.* **124**, 243–249 (1929).
63. Evanse, V., Kenney, C. N. Gaseous Dispersion in Laminar Flow Through a Circular Tube, *Proc. Roy. Soc. A.* **284**, 540-550 (1965).
64. Caro, C. G. The dispersion of indicator flowing through simplified models of the circulation and its relevance to velocity profile in blood vessels, *J. Physiol.* **185**, 501-519 (1966).
65. Erdogan, M.E., Chatwin, P.C. The effects of curvature and buoyancy on the laminar dispersion of solute in a horizontal tube, *J. Fluid. Mech.*, **29**, 465-484 (1967).
66. Nunge, R.J., Lin, T.S., Gill, W.N. Laminar dispersion in curved tubes and channels, *J. Fluid. Mech.*, **51**, 363-383 (1972).
67. Topakoglu, H.C. Steady laminar flows of an incompressible viscous fluid in curved pipes, *J. Match. Mech.*, **16**, 1321-1338 (1967).
68. Janssen, L.A.M. Axial dispersion in laminar flow through coiled tubes, *Chem. Eng. Sci.*, **31**, 215-218 (1976).
69. Agrawal, S., Jayaraman, G. Numerical simulation of dispersion in the flow of power law fluids in curved tubes, *Appl. Math. Modelling*, **18**, 504-512 (1994).
70. Johnson, M., Kamm, R. Numerical studies of steady flow dispersion at low Dean number in a gently curving tube, *J. Fluid Mech.*, **172**, 329–345 (1986).

71. Ye, F., Jensen, H., Larsen, S. W., Yaghmur, A., Larsen, C., Østergaard, J. Measurement of drug diffusivities in pharmaceutical solvents using Taylor dispersion analysis, *J. Pharm. Biomed. Anal.* **61**, 176–183 (2012).
72. Wilke, C. R., Chang, P. Correlation of diffusion coefficients in dilute solutions, *AIChE J.* **1**, 264–270 (1955).
73. Kalwarczyk, T., Tabaka, M., Hołyst, R. Biologistics—Diffusion coefficients for complete proteome of *Escherichia coli*, *Bioinformatics*, **28**, 2971–2978 (2012).
74. Corless, R. M., Gonnet, G. H., Hare, D. E. G., Jeffrey, D. J., Knuth, D. E. On the Lambert W Function, *Adv. Comput. Math.* **5**, 329–359 (1996).
75. Brune, D., Kim, S. Predicting protein diffusion coefficients, *Proc. Natl. Acad. Sci. U.S.A.*, **90**, 3835–3839 (1993).
76. Nauman, J. V., Campbell, P. G., Lani, F., Anderson, J. L. Diffusion of insulin-like growth factor-I and ribonuclease through fibrin gels, *J. Biophys.*, **92**, 4444–4450 (2007).
77. Daniel, V., Albright, J. G. Measurement of mutual-diffusion coefficients for the system KNO₃–H₂O at 25°C, *J. Solution Chem.*, **20**, 633–642 (1991).
78. Lewandrowska, A., Majcher, A., Ochab-Marcinek, A., Tabaka, M., Hołyst, R. Taylor dispersion analysis in coiled capillaries at high flow rates, *Anal. Chem.* **85**, 4051–4056 (2013).
79. Danquah, M. K., Agyei, D. Pharmaceutical applications of bioactive peptides. *OA Biotechnol.*, **1**, 1-7 (2012).
80. Hawe, A., Hulse, W. L., Jiskoot, W. and Forbes, R. T. Taylor Dispersion Analysis Compared to Dynamic Light Scattering for the Size Analysis of Therapeutic Peptides and Proteins and Their Aggregates, *Pharm. Res.* **28**, 2302–2310 (2011)
81. Santos, S., Torcato, I., Castanho, M. A. R. B. Biomedical applications of dipeptides and tripeptides, *Biopolymers*, **98**, 288–293 (2012).
82. Amidon, G.L., Lee, P.I., Topp, E.M. *Transport Processes in Pharmaceutical Systems*, Marcel Dekker (2000).
83. Bikard, D., Loot, C., Baharoglu, Z., Mazel, D. Folded DNA in Action: Hairpin Formation and Biological Functions in Prokaryotes, *Microbiol. Mol. Biol. Rev.* **74**, 570–588 (2010).

84. Mariappan, S. V. S., Catasta, P., Chen, X., Ratliff, R., Moyzis, R. K., Bradbury, E. M., Gupta, G. Solution structures of the individual single strands of the fragile X DNA triplets (GCC)_n(GGC)_n, *Nucleic Acids Res.* **24**, 784-792 (1996).
85. Amir-Aslani, A., Mauffret, O., Bittoun, P., Sourgen, F., Monnot, M., Lescot, E., Femandijan, S. Hairpins in a DNA site for topoisomerase II studied by ¹H- and ³¹P-NMR, *Nucleic Acids Res.* **23**, 3850-3857 (1995).
86. Chen, X., Mariappan, S. V., Catasti, P., Ratliff, R., Moyzis, R. K., Laayoun, A., Smith, S. S., Bradbury, E. M., Gupta, G. Hairpins are formed by the single DNA strands of the fragile X triplet repeats: Structure and biological implications, *Proc. Natl. Acad. Sci.* **92**, 5199-5203 (1995).
87. Haasnoot, C.A., Hilbers, C.W., van der Marel, G.A., van Boom, J.H., Singh, U.C., Pattabiraman, N., Kollman, P.A. On loop folding in nucleic acid hairpin-type structures, *J. Biomol. Struct. Dyn.*, **3**, 843-857 (1986).
88. Wemmer, D.E., Chou, S.H., Hare, D.R., Reid, B.R. Duplex-hairpin transitions in DNA: NMR studies on CGCGTATACGCG, *Nucleic Acids Res.*, **13**, 3755-3772 (1985).
89. Jung, J., van Orden, A. Folding and Unfolding Kinetics of DNA Hairpins in Flowing Solution by Multiparameter Fluorescence Correlation Spectroscopy, *J. Phys. Chem. B* **109**, 3648-3657 (2005).
90. Jung, J., Van Orden, A. A three-state mechanism for DNA hairpin folding characterized by multiparameter fluorescence fluctuation spectroscopy, *J. Am. Chem. Soc.* **128**, 1240-1249 (2006).
91. Kim, J., Doose, S., Neuweiler, H., Sauer, M. The initial step of DNA hairpin folding: A kinetic analysis using fluorescence correlation spectroscopy, *Nucleic Acids Res.* **34**, 2516-2527 (2006).
92. Kuzmanovic, D. A., Elashvili, I., Wick, C., O'Connell, C., Krueger S. Bacteriophage MS2: Molecular Weight and Spatial Distribution of the Protein and RNA Components by Small-Angle Neutron Scattering and Virus Counting, *Structure*, **11**, 1339-1348 (2003).
93. King, A. M.Q., Adams, M. J., Lefkowitz, E. J. *Virus Taxonomy*, Elsevier (2012).
94. Northrop, R. B., Connor, A. N. *Introduction to Molecular Biology, Genomics and Proteomics for Biomedical Engineers*, CRC Press (2009).

95. Creighton, T. E. *Proteins: Structures and Molecular Properties*, W. H. Freeman and Company (1993).
96. Branden, C., Tooze, J. *Introduction to Protein Structure*, Garland Publishing Inc. (1999).
97. Leja, D. *Talk. Gloss. Genet. Terms*, www.genome.gov/Glossary/resources/protein.pdf, accessed August 2013.
98. Bennion, B. J., Daggett V. The molecular basis for the chemical denaturation of proteins by urea, *PNAS*, **100**, 5142-5147 (2003).
99. Raymond F. Greene, Jr. and C. Nick Pace, Urea and Guanidine Hydrochloride Denaturation of Ribonuclease, Lysozyme, α -Chymotrypsin, and β -Lactoglobulin, *J. Biol. Chem.* **249**, 5388-5393 (1974).
100. T. Matsumoto and H. Inoue, Effect of heat denaturation on the structure and rheological properties of ovalbumin aqueous colloids, *J. Chem. Soc. Faraday Trans.* **87**, 3385-3388 (1991).
101. Sawyer, W.H. Heat Denaturation of Bovine β -Lactoglobulins and Relevance of Disulfide Aggregation, *J. Dairy Sci.*, **51**, 323-329 (1968).
102. Dobson, M.Ch., Protein folding and misfolding, *Nature*, **426**, 18-25 (2003).
103. Kelly J. The alternative conformation of amyloidogenic proteins and their multistep assembly pathways, *Curr. Opin. Struct. Biol.* **8**, 101-106 (1998).
104. Valstar, A., Almgren, M., Brown, W., Vasilescu, M. The Interaction of Bovine Serum Albumin with Surfactants Studied by Light Scattering, *Langmuir* **16**, 922-927 (2000).
105. Valstar, A., Brown, W., Almgren, M. The Lysozyme-Sodium Dodecyl Sulfate System Studied by Dynamic and Static Light Scattering, *Langmuir* **15**, 2366-2374 (1999).
106. Vasilescu, M., Angelescu, D., Almgren, M., Valstar, A. Interactions of globular proteins with surfactants studied with fluorescence probe methods, *Langmuir* **15**, 2635-2643 (1999).
107. Zhang, X., Poniewierski, A., Hou, S., Sozański, K., Wiśniewska, A., Wieczorek, S., Kalwarczyk, T., Sun, L., Hołyst, R. Tracking structural transitions of bovine serum albumin in surfactant solutions by fluorescence correlation spectroscopy and fluorescence lifetime analysis. *Soft Matter* **11**, 2512-2518 (2015).

108. Tah, B., Pal, P., Talapatra, G. B. Interaction of insulin with SDS/CTAB cationic Vesicles, *J. Lumin.* **145**, 81–87 (2014).
109. Tejaswi Naidu, K., Prakash Prabhu, N. Protein-surfactant interaction: Sodium dodecyl sulfate-induced unfolding of ribonuclease A. *J. Phys. Chem. B* **115**, 14760–14767 (2011).
110. Nielsen, M. M., Andersen, K. K., Westh, P., Otzen, D. E. Unfolding of β -Sheet Proteins in SDS, *Biophys. J.* **92**, 3674–3685 (2007).
111. Otzen, D. Protein-surfactant interactions: A tale of many states, *Biochim. Biophys. Acta*, **1814**, 562–591 (2011).
112. Yuan, C. L., Xu, Z. Z., Fan, M. X., Liu, H. Y., Xie, Y. H., Zhu, T. Study on characteristics and harm of surfactants, *J. Chem. Pharm. Res.*, **6**, 2233–2237 (2014).
113. Fendler, J. H., Fendler, E. J. *Catalysis in Micellar and Macromolecular Systems*, Academic Press (1975).
114. Quina, F. H., Nassar, P. M., Bonilha, J. B. S., and Bales, B. S., Growth of Sodium Dodecyl Sulfate Micelles with Detergent Concentration, *J. Phys. Chem.* **99**, 17028–17031 (1995).
115. Romani, A. P., da Hora Machado, A. E., Hioka, N., Severino, D., Baptista, M. S., Codognoto, L., Rodrigues, M. R., and de Oliveira, H. P., Spectrofluorimetric Determination of Second Critical Micellar Concentration of SDS and SDS/Brij 30 Systems. *J. Fluoresc.*, **19**, 327–332 (2009).
116. Turro, N. J., Lei, X.-G., Ananthapadmanabhan, K. P., Aronson, M. Spectroscopic Probe Analysis of Protein-Surfactant Interactions: The BSA/SDS System, *Langmuir*, **11**, 2525–2533 (1995).
117. Geissler, E. *Dynamic Light Scattering from polymer gels*. Brown W. *Dynamic Light Scattering. The method and some applications*, Calendron Press, (1993).

B. 488/16



Biblioteka Instytutu Chemii Fizycznej PAN

F-B.488/16



40000000199252